D.T3.2.1 Report on “Preparation for risk analysis and strategy workshops”

GREEN RISK 4 ALPS

WP 3

Responsibility for Deliverable

Silvia Cocuccioni (Eurac Research)

Contributors

Kathrin Renner, Stefan Steger (Eurac Research)
Christopher D’Amboise, Anne Hormes, Matthias Plörer, Michaela Teich (BFW)

Bolzano, September 2020

GreenRisk4ALPs Partnership

BFW - Austrian Research Centre for Forests (AT)
DISAFA - Department of Agricultural, Forest and Food Sciences, University of Turin (ITA)
EURAC - European Academy of Bozen-Bolzano – EURAC Research (ITA)
INRAE – French national research institute for agriculture, food and the environment, Grenoble regional centre (FRA)
LWF - Bavarian State Institute of Forestry (GER)
MFM - Forestry company Franz-Mayr-Melnhof-Saurau (AT)
SFM - Safe Mountain Foundation (ITA)
UL - University of Ljubljana, Biotechnical Faculty, Department of Forestry and Renewable Resources (SLO)
UGOE - University of Göttingen, Department of Forest and Nature Conservation Policy (GER)
WSL - Swiss Federal Institute for Forest, Snow and Landscape Research (CH)
WLV - Austrian Service for Torrent and Avalanche Control (AT)
SFS - Slovenia Forest Service (SLO)

Table of Contents

Table of Figures

Table of Tables

1. Introduction

The project *GreenRisk4ALPs* aims to develop ecosystem-based approaches to support risk management of the Alpine region. In particular, the project focuses on gravitational mass movements, such as landslides, rock falls and snow avalanches. In order to develop a successful ecosystem-based risk management strategy, natural hazard processes and their potential consequences need to be studied; moreover, analysing how these hazards are currently managed is a prerequisite to understand how to improve the risk management of the future.

This deliverable is a part of Activity A.T.3.2 and provides an overview of the methodologies adopted as inputs for the risk analysis, carried out within Work Package 3. After a brief explanation on how the concept of risk is used within the project (Chapter 1), we present an overview of the different methodologies, objectives of this deliverable, which feed into the risk analysis. Chapter 2 focuses on the Rapid Risk Appraisal concept and method. Subsequently, the spatial analysis is presented in Chapter 3, providing an overview of the elements needed for its implementation (i.e. spatial hazard models: Chapter 3.1; asset data and maps: Chapters 3.2.1-3.2.2).

The "Risk" concept within GreenRisk4Alps

Natural hazards are events capable of threatening exposed assets and people, leading to human, material, economic and environmental impacts and losses. The potential for such negative impacts to happen is often referred to as risk (IPCC, 2014; UNDRR, 2009). When hazardous events have a major impact on the functioning of a community or a society, they can also be defined as disasters (Alcántara-Ayala, 2002). Risk is indeed defined differently by different scientific communities. In GreenRisk4Alps, we try to bridge the definitions used in the Climate Change Adaptation (CCA) and Disaster Risk Reduction (DRR) communities, by adopting the risk concept of the Fifth Assessment Report (AR5) of the IPCC Working Group II. In this concept, risk is a result of the interaction of vulnerability, exposure, and hazard (IPCC, 2014; See Box 1). Risks derive from the combination of natural hazards and the vulnerabilities of exposed elements. In other words, the hazard itself does not constitute a risk if it occurs in an area where no assets or people are present; moreover, not all the elements exposed to a hazard are necessarily vulnerable (Cardona et al., 2012)

Box 1: Definitions of "Risk" and its components

Risk:

"*The potential disaster losses, in lives, health status, livelihoods, assets and services, which could occur to a particular community or a society over some specified future time period*" (UNDRR, 2009, p.9).

"*The potential loss of life, injury, or destroyed or damaged assets which could occur to a system, society or a community in a specific period of time, determined probabilistically as a function of hazard, exposure, vulnerability and capacity*" (IPCC, 2014, p.40)

Hazard: *"The potential occurrence of a natural or human-induced physical event that may cause loss of life, injury, or other health impacts, as well as damage and loss to property, infrastructure, livelihoods, service provision, and environmental resources"* (IPCC, 2014, p.39)

Exposure: "*The presence of people; livelihoods; environmental services and resources; infrastructure; or economic, social, or cultural assets in places that could be adversely affected*" (IPCC, 2014, p.39)

Vulnerability: *"The propensity or predisposition to be adversely affected. Vulnerability encompasses a variety of concepts including sensitivity or susceptibility to harm and lack of capacity to cope and adapt*." (IPCC, 2014, p.39)

In order to assess and to subsequently manage or reduce risks, the three risk components need to be analysed. The approach adopted in GreenRisk4Alps is illustrated in Figure 1. Spatial **natural hazard** models were developed within Work Package 1. A focus was put on the understanding of where the forest plays a role in reducing the impact of a natural hazard. Spatially explicit information on assets such as linear infrastructure and buildings were collected within Work Package 2 (see also Deliverable D.T.2.4.2 for more information) and used to select exposure hotpots in Work Package 3. Moreover, information from local experts was acquired through the Rapid Risk Appraisal (RRA), a participatory process which focuses on analysing how the different Pilot Action Regions (PARs) currently cope with the potential natural hazards and respective risks by preventing, mitigating, avoiding, lessen or transferring their adverse effects. While the hotspot analysis focuses on the exposure component of risk, the RRA concentrates on the capacity to cope and adapt, which is often considered as a vulnerability factor (IPCC, 2014). Assessing the presence (or the lack) of capacities constitutes the basis to achieve the overall aim of the project: improving the risk management of the PARs through the implementation of ecosystem-based approaches.

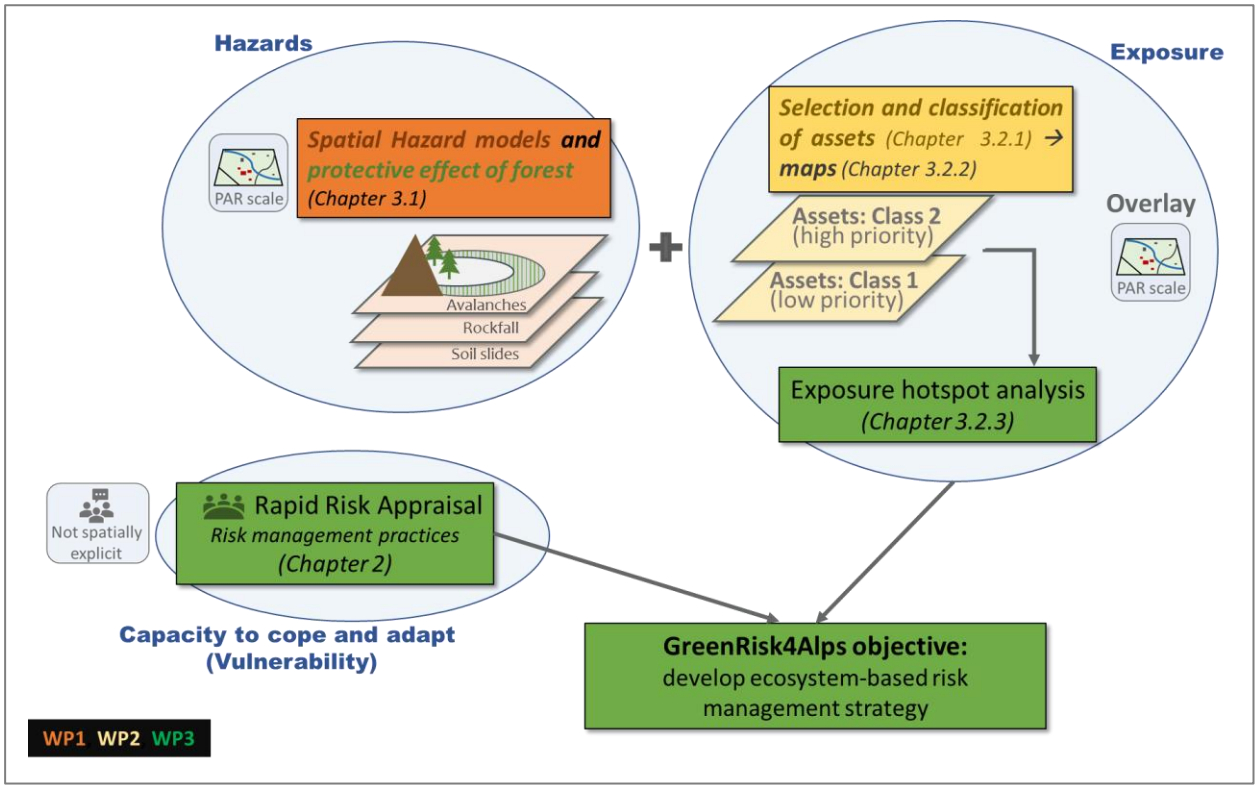

Figure 1: Approach adopted for the risk analysis within GreenRisk4Alps. The respective chapters which address each method are also reported.

2. Rapid Risk Appraisal (RRA)

The RRA is a participatory tool which aims to identify the strengths and the points for improvement in the field of risk management in the different PARs for the implementation of future risk reduction measures. Consequently, this tool aims at supporting municipalities to increase their resilience to natural disasters.

The RRA makes use of local knowledge through the involvement of local experts in a short (few hours to half-day), collaborative workshop. This way, qualitative information as well as detailed knowledge on local particularities can be collected in a short time frame within a group setting. The personal information exchange which takes place through such a participatory approach also fosters mutual learning and information exchange among experts with a diverse technical background. The results gained from this participatory exercise can serve as a starting point for a more in-depth analysis, providing also a more specific direction in which to focus the detailed spatially explicit risk assessment and scientific research in general.

The RRA methodology focuses on assessing parts of the vulnerability component of risk. Vulnerability is defined by the IPCC (2014, p. 39) as "*the propensity or predisposition to be adversely affected. Vulnerability encompasses a variety of concepts including sensitivity or susceptibility to harm and lack of capacity to cope and adapt*". Vulnerability is therefore composed of two elements: **sensitivity** and **capacity** (GIZ and EURAC, 2017). The first refers to the physical attributes of a system (i.e. building material of buildings), social, economic and cultural attributes (i.e. age, income). The latter, capacity, describes the ability of societies to prepare for and respond to current and future natural hazard impacts (GIZ and EURAC, 2017). The RRA focuses on the assessment of the second, particularly concentrating on the local risk management capacities in place in the different PARs.

Risk management is defined as a systematic process for the inclusive treatment of risks (FOCP, 2014). It includes measures to systematically identify and assess risks. It also includes directed communication about hazards and their related risks, as well as relevant response, monitoring and recovering measures (FOCP, 2014). It is therefore important to underline that the RRA approach is not a conventional risk assessment methodology as it does not focus on analysing the interactions between the three risk components (natural hazard, exposure and vulnerability). It is instead aimed at assessing the availability and quality of different activities carried out to understand, prevent, respond to and recover from potential risks, among which risk assessment is one.

The experts to be invited to the RRA workshop are selected in collaboration with the PAR responsible partners. The selection of participants aims to provide both technical and applied expertise within the field of risk management (e.g. geology department, torrent and avalanche control experts but also foresters, civil protection, land use planners and municipality technicians). Moreover, different technical experts should be present, covering a range of gravity-driven natural hazards. In each PAR responsibilities in risk management differ; therefore, the stakeholder network analysis carried out in D.T.2.2.2 will provide a valuable input to select the most suitable experts. Overall, five to ten experts will be selected for each PAR.

The RRA approach follows a series of steps, adapted from the ISO standard 31000 for risk management (Figure 2). The standard focuses on providing guidelines for the management of risks. Although it mainly addresses organisations and industries, it can be customised and applied to different activities, including decision-making at all levels (International Standard Organisation, 2018). ISO3100 is here applied as a general framework to guide the collection of information during the workshop. The three steps are the following: risk identification (1), risk analysis (2), risk evaluation (3).

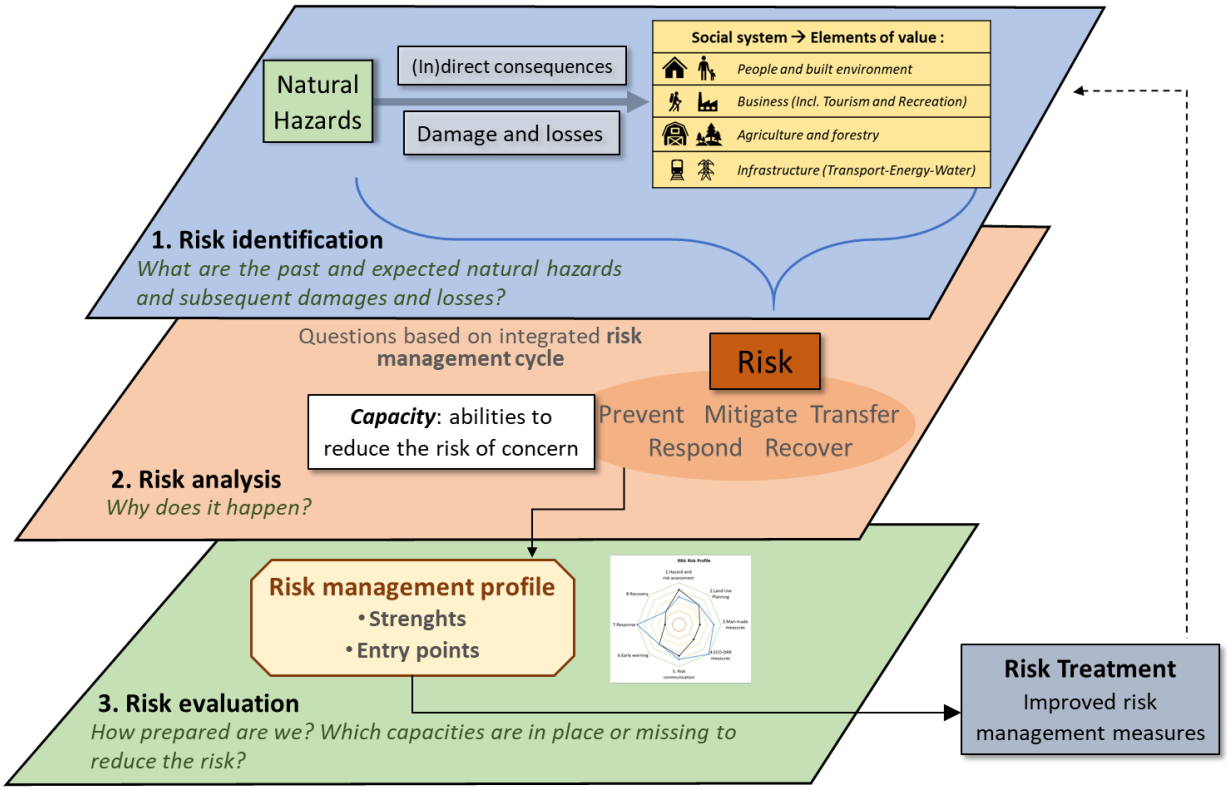

Figure 2: The three RRA steps, adapted from ISO 31000

Risk identification (step 1)

This step aims at identifying the two natural hazards which are the most relevant from a risk perspective for each PAR. Thus, the focus of this step is discussing about damage and losses that the different hazards have caused in the past and which are likely to cause in the future. The indirect consequences caused by such events (i.e. impact on reputation, interruption of activities) are also addressed. Consequently, this step provides information about the general sensitivity to natural hazards starting from the lessons we can learn from the past and moving on to potential and future risks. As suggested by ISO 31000, the discussion is carried out in a systematic and collaborative way using open ended questions that allow the interviewees to describe the key natural processes which affect the area (International Standard Organisation, 2018). In order not to miss any relevant point, the discussion of the risk identification phase follows a pre-defined list of sectors (see Table 1).

Table 1: List of sectors to be addressed during the discussion about past and potential damage and losses

Sectors
People and built environment
Business (Incl. Tourism and Recreation)
Agriculture and forestry
Infrastructure (Transport-Energy-Water)

The questions listed in Table 2, adapted from the Risk Supplement to the Vulnerability Sourcebook (GIZ and EURAC, 2017), are adopted as a guideline to guide the group discussion. Moreover, maps are also used to visualise the areas mentioned by the different experts. If available, maps can include past natural hazard events or hazard zone plans.

Table 2: Questions to guide the discussion in the first step of the RRA (risk identification)

Past	➢ Which natural hazards caused damage and/or fatalities or were "near hits" for each sector? ➢ How have the natural hazards impacted directly and indirectly the sectors? What type of damage happened?
Future	➢ Which natural hazard events and their direct physical impacts pose a risk in each sector? ➢ What type of damage and losses are expected?

Risk analysis (step 2)

The Risk Analysis step builds on the previous discussion and represents the core of the RRA.
The aim of this step is therefore to analyse risk management practices in place in the PAR, related to the two previously selected natural hazards. In order to cover all the risk management activities, questions are structures following the Integrated Risk Management cycle steps (See Figure 3; FOCP, 2014). Integrated risk management is understood as a holistic and integrated approach to risk management in which different types of measures for natural risk reduction are considered as equally important. The adopted measures should therefore cover the preparedness, the response and the recovery phases (Mikoš, 2013).

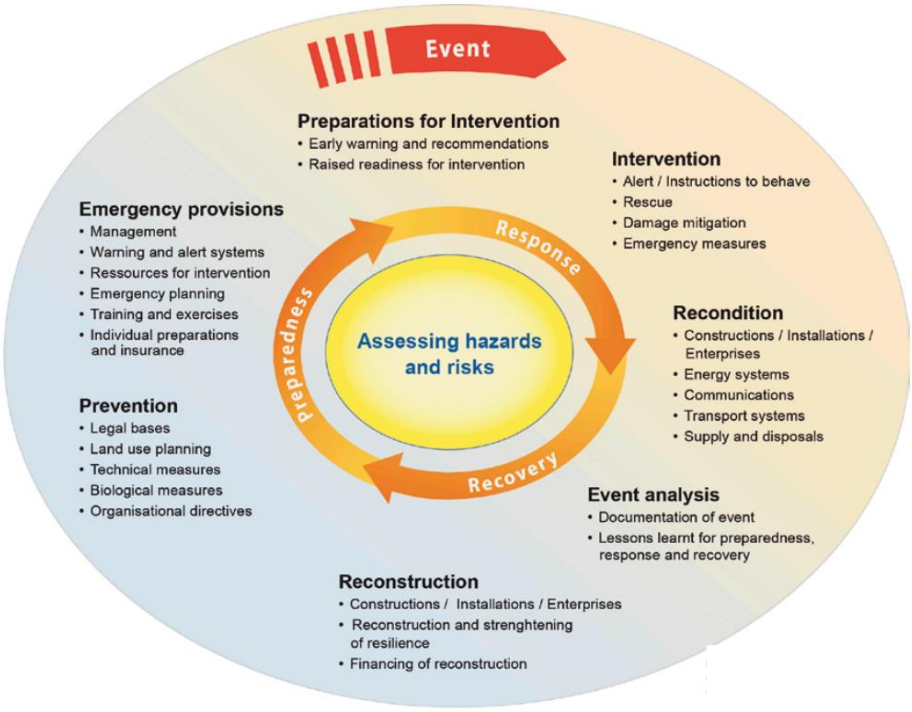

Figure 3: The Integrated Risk Management Cycle used to structure the RRA questions, in order to cover all the possible measures, capabilities in place to be analysed (FOCP, 2014)

The selected questions which constitute this step of the RRA are divided in eight categories and are listed in Table 3 below.

Table 3: Questions for the RRA analysis step. They are divided into seven categories and cover the different steps or components of the Integrated Risk Management Cycle. Note that each question is presented together with three possible answers which correspond to different scenarios of expert satisfaction. A complete example of a question and its proposed answers is available in ***Fehler! Verweisquelle konnte nicht gefunden werden.****.*

#	Category	Questions /indicators	
1	Hazard and risk assessment	1.1	Is a database of past NH events available?
2		1.2	Are maps showing likelihood of occurrence of natural hazards available for the area? (i.e. susceptibility/ hazard map)
3		1.3	Are local administrations aware of which assets and people are exposed to NHs? How do you know which asset(s) is/are exposed to natural hazards?
4	Land Use / Urban Planning	2.1	Are risks / hazards accounted for in land use planning? (i.e. hazard zone plans legally binding)
5	Man-made measures	3.1	Is an inventory of technical measures available?
6		3.2	Are technical measures maintained following an official plan?

7		3.3	Are risk reduction actions taken as a consequence of natural hazard monitoring/ forecasting? (before hazard occurs) (i.e. controlled explosions, evacuations of houses)
8	ECO-DRR measures	4.1	Are protection forests maps available?
9		4.2	Are protection forests recognised and protected by law? (i.e. no land use change allowed, compulsory sylvicultural actions?)
10		4.3	Are protection forests included/ accounted for in hazard/risk assessment?
11	Risk communication	5.1	Is the public informed through a diversity of channels? (i.e. social media, signs, traditional media etc)
12		5.2	Are natural hazards and their related risks part of primary / secondary school educational programs?
13		5.3	Do risk communication activities address audiences speaking different languages?
14		5.4	Are the results of risk communication activities assessed? Does anyone verify if people respond correctly?
15	Early warning	6.1	Are alert systems for the population available? (i.e. sms)
16		6.2	Are automatic detection systems available? (i.e. avalanche radar)
17	Response	7.1	Are damages and fatalities promptly and systematically assessed?
18		7.2	Is a formal emergency plan adopted?
19		7.3	Are simulations/tests of emergency response carried out?
20	Recovery	8.1	Are assets and/or people covered by insurance against the natural hazard of concern?
21		8.2	Are damages promptly addressed?
21		8.3	Are past experiences systematically used to improve risk management of the future?
23	CCA	Extra	Is a climate change adaptation strategy/plan available at regional/municipal level ?

Each of the questions listed above is presented together with three possible answers which correspond to different scenarios of expert satisfaction.The first scenario describes the case in which the participants perceive the specific risk management practice as a best practice or if they are highly satisfied with its quality or implementation. On the contrary, the third scenario, foreses a low expert satisfaction and ample room for improvement. The second scenario provides the intermediate or average case, where experts see space for desiderable improvements. Along with the three scenarios, discussion points such as concrete best practice examples of the Alps are listed to provide existent examples or comparisons to which experts could refer to during the discussion. The different experts are asked to answer and discuss each question in detail,

explaining how each risk management-related-practice functions in their PAR, considering the differences and similarities for both the selected natural hazards. Finally, experts are asked to come to an agreement and to select one of the three proposed scenarios.

Furthermore, different scores are attributed to the three scenarios. The maximum number of points is assigned to the best practice scenario (scenario one); on the contrary, the least is given in case some points are missing and an improvement is considered as necessary (scenario three). The full answer, the selected scenarios and the respective points are all recorded and used in the risk evaluation step.

An example of a question, the scenarios and respective discussion points are provided below (Figure 4).

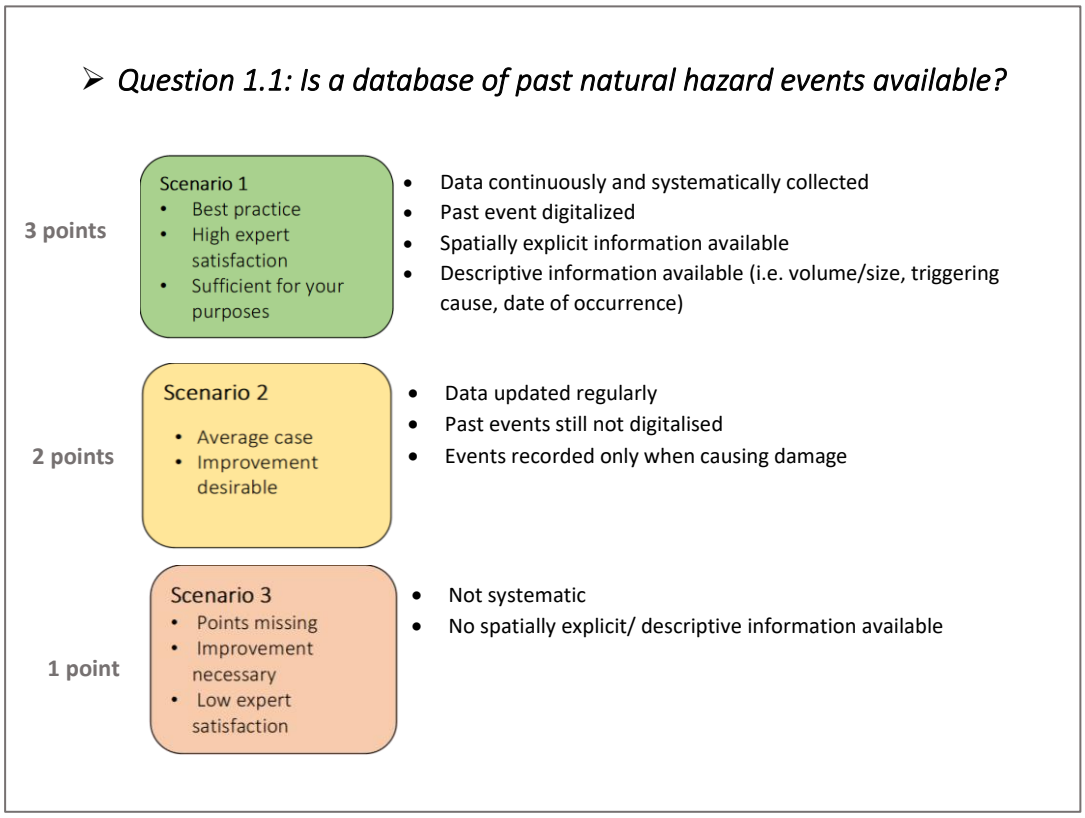

Figure 4: An example of a question of the RRA, including scenarios on which the experts should agree on and possible discussion points attributed to each scenario. On the left also the points assigned to each scenario are reported.

Risk evaluation (step 3)

The points assigned in the previous steps are used to generate a spider chart. For this scope, the assigned points are inserted in an Excel Sheet and the average for each category is then calculated.

The spider chart, called here **Risk (management) Profile,** allows to easily compare different natural hazards and various study areas (see Figure 5). The larger the area of the polygon (different colour lines for each hazard), the more the activities in the field of risk management are considered as best practices by the participants.

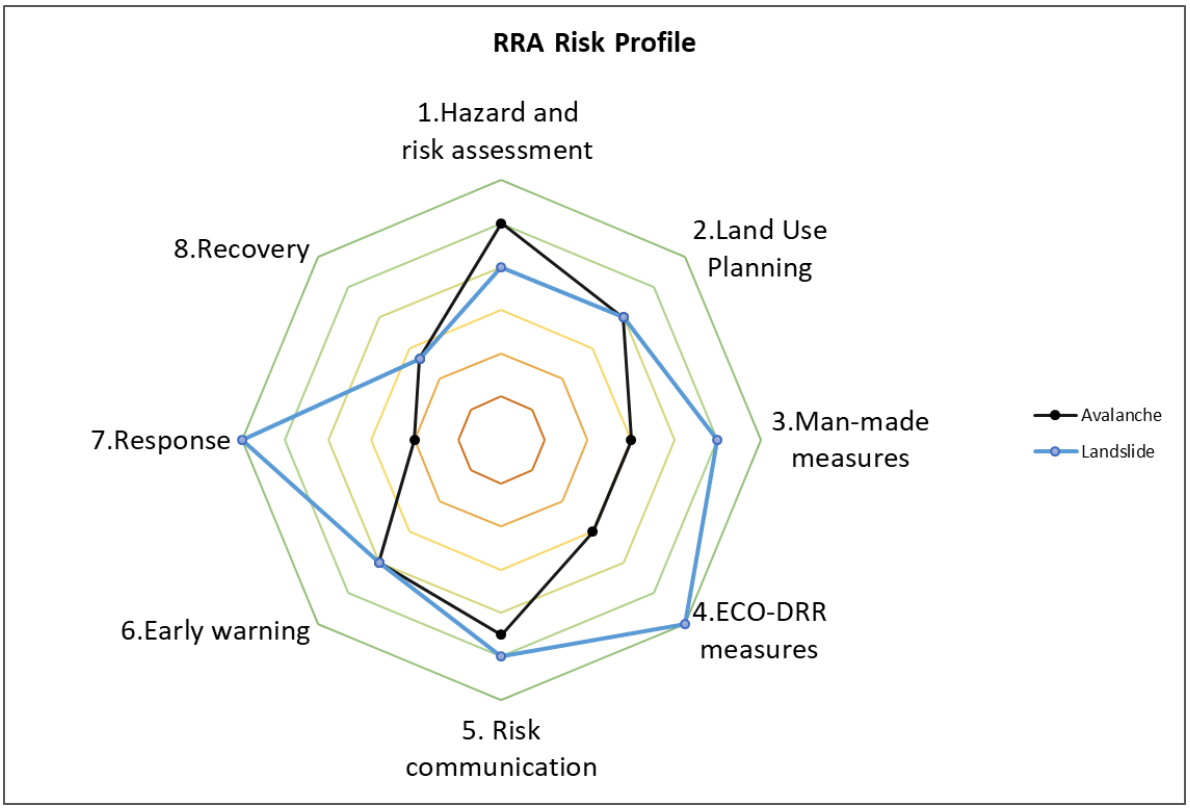

Figure 5: Example of a Risk (management) profile. a spider chart that allows to compare the risk management capacities in place related to different natural hazards

The spider chart is presented and discussed with the participants as a final step of the workshop. By presenting the Risk Management Profile, the participants receive an immediate picture which summarises the RRA risk management practices addressed during the half-a-day workshop. This way, the strengths in risk management can be underlined and entrance points for improvement can be summarised.

Finally, after the execution of the RRA workshops in the different study areas, the results from different PARs are compared, considering not only the Profile but also the full recorded answers. Best practices or strengths which arise from the analysis of the results of one PAR could be transferred or proposed to PARs presenting specific weaknesses. This way, one PAR can learn from the risk management of the others and a more successful ecosystem-based strategy can be proposed within the project. In particular, the final results of the RRA activity will be presented in D.T.3.5.1.

3. Spatial analysis of exposure hotspots

The spatial identification of exposure hotspots is complementary to the previously presented RRA approach (Chapter 2). The RRA elaborates strengths and improvement potential in risk management using a participatory approach whereas the analysis of exposure hotspots uses GIS-based modelling tools to identify areas where the forest can play a role in protecting infrastructure from various gravity-driven hazards. Instead of focusing on single slopes and single infrastructures, the analysis design relates to the regional scale in order to provide maps that cover the entire PAR. The general idea is to combine spatial hazard models that account for the protective effect of forest (3.1) with information on exposed elements (3.2) in order to identify hotspots where the current forest is relevant to reduce a potential hazard impact (3.2.3). Chapter 3 presents the methodical workflow while the ensuing results for each PAR are described within deliverable D.T.3.5.1.

3.1. Spatial hazard models and protective effect of forest

This section describes the general workflow to produce the spatially explicit hazard models for the three processes of interest, namely landslides (3.1.2), snow avalanches (3.1.3). rockfall (3.1.4). The Flow-py model is introduced first (3.1.1), since all hazard specific models described below include or built-upon this GIS-based modelling framework.

3.1.1. Introduction to Flow-py

The Flow-py model is a flexible GIS-based regional scale gravitational hazard (rockfall, snow avalanche and shallow landslide) runout model that was developed at the Austrian Research Centre for Forests (BFW). To maximize its applicability, the Flow-py model was developed to utilize simple input data that is flexible with regards to data quantity and information depth (data level), and widely available for many regions of the world, i.e. it only requires a digital elevation model (DEM) and a raster that specifies process release areas (see D.T1.2.3 and D.T.1.3.3).

The Flow-py model can be split into two major routines, the routing algorithm and the stopping criteria. Flow-py employs a routing algorithm that relies on past modelling concepts (Holmgren, 1994; Horton et al., 2013; Gamma, 1999), and on an improved hazard routing in flat or uphill terrain. There are two stopping criteria that are employed: the first is a runout angle criterion that limits how far the process travels dependent on the local topography (Figure 6b). The second is based on the overall susceptibility (Horton et al., 2013), which limits the lateral spreading of the mass as it travels down slope.

Figure 6a shows the workflow of the Flow-py model as used by the avalanche process in GR4A. The minimum data requirements needed to run Flow-py are a DEM and a release area layer. For the case of avalanches, the DEM and information on yearly maximum mean snow depths were used to determine potential release pixels (see Section 0 for details). The results of the Flow-py model are raster files that show the process runout and additional supporting raster layers that can be used in post-processing steps. For the GR4A project, we used 10-m resolution raster files. DEMs in 10 m resolution are widely available and allow to model gravitational hazard processes in the resolution and detail level needed for regional applications.

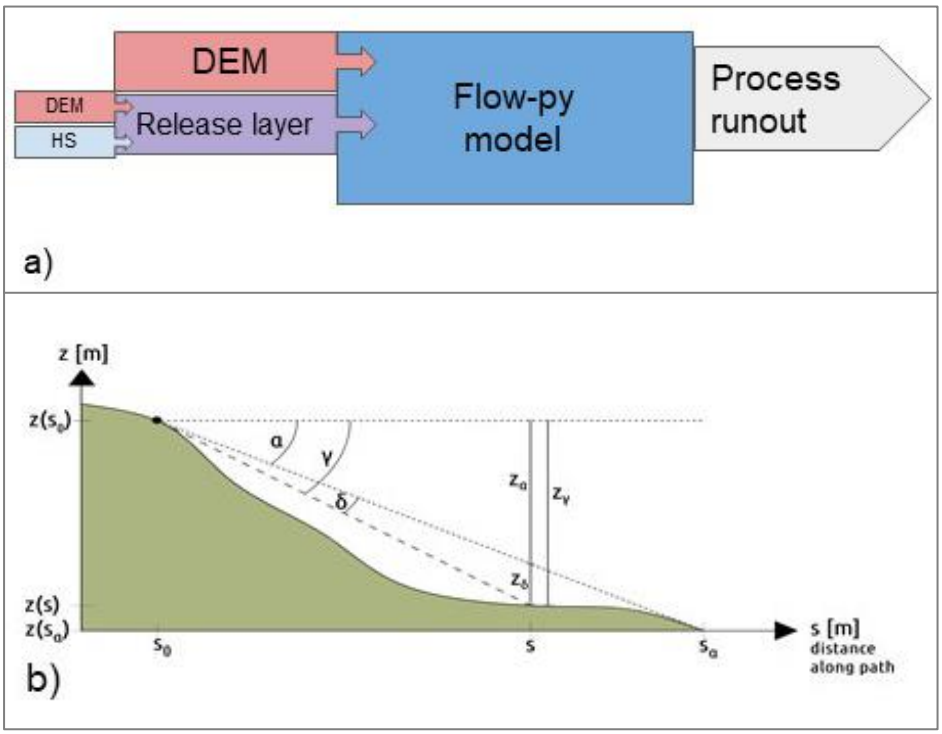

Figure 6: a) Workflow of the Flow-py model as used for the snow avalanche process in GR4A; HS = snow depth, DEM = digital elevation model. b) Flow-py runout modeling principle, which is an angle stopping criterion (one of the two stopping criteria), where α is the runout angle, which is determined and predefined for each hazard process, γ is the local angle, which is calculated stepwise for each raster cell dependent on the local topography, and δ is the difference between the two (γ - α). If δ ≤ 0, then the hazard process stops. These same equations can be derived from basic physical models assuming only Coulomb friction, which allows to interpret zδ (ELH = energy line height) as the potential and kinetic energy of the system.

We chose to apply the simple empirical-based Flow-py model instead of a more sophisticated and data demanding process-based physical models in GR4A, because:

- There is a need for model flexibility in terms of input data quantity, information depth and resolution, because the input data is supplied by many different countries, states and institutions resulting in different input data qualities.
- Empirical models are generally less computationally expensive and can therefore be applied over regional modelling domains.
- The empirical approach for runout models requires fewer parameterizations when compared to process-based physical models. Therefore, parameterization of Flow-py is relatively simple and outputs are better comparable between modelling regions.

Flow-py was developed in the Python 3 computer language and designed to allow for the integration of custom-made plugins, which enables users to adapt the model to address a specific question. Plugins can require more input data, adapt the output layers, and even change what and how the model computes. For GR4A two plugins were created to address the specific needs of the project: 1) the back-calculation plugin, and 2) the forest plugin.

1) The **back-calculation plugin** identifies the process paths that interact with infrastructure (elements at risk;
2) Figure 7). The back-calculation plugin requires an infrastructure GIS layer; in GR4A we used a 10-m resolution raster file with locations of building, transportation and recreational infrastructure and infrastructure classes (see D.T2.4.2 for details). The back calculation represents a spatially explicit subset of the process runout. If a process path includes a raster cell with infrastructure, then the back calculation identifies every path the mass could take (from raster cell to raster cell) from the infrastructure to the associated starting cell. Every raster cell identified by the back calculation as related to endangering infrastructure has information about the infrastructure class saved in the output raster. That means that the back calculation highlights the location of hazard starting zones and process paths associated with endangering infrastructure. Furthermore, the back calculation classifies the highlighted process areas with regards to the class of infrastructure that is endangered (see D.T2.4.2). The result as the process runout with back calculation can then be overlaid with a map of the forest cover extent to identify forest areas with a direct object protective function (Direct Object Protection Forest; see D.T1.4.1 for definition).

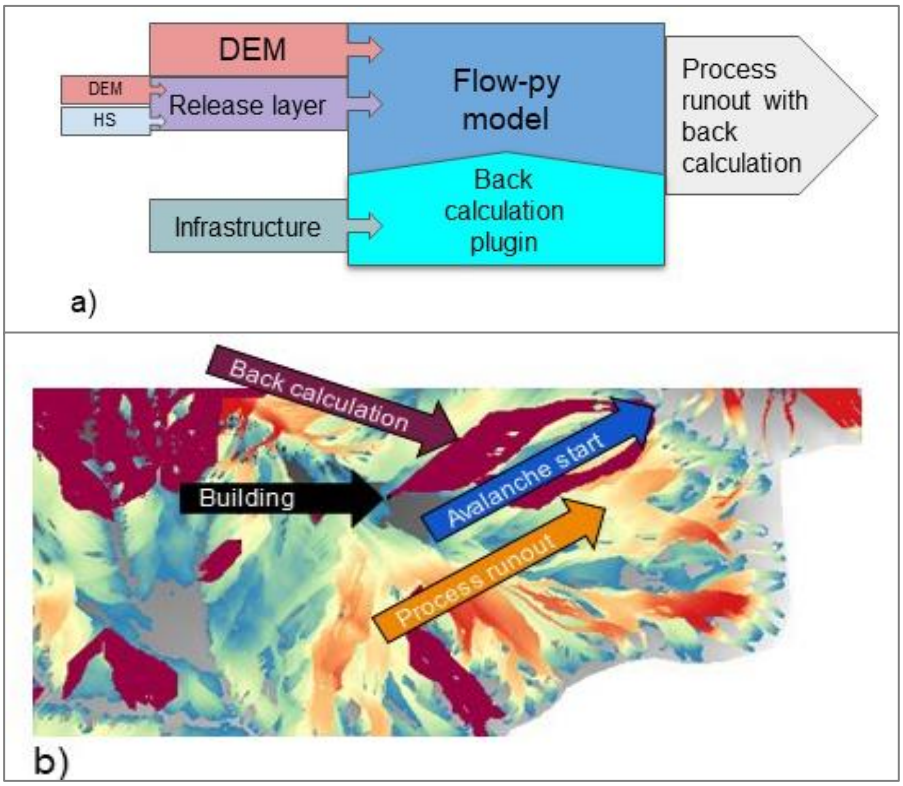

Figure 7. a) Workflow of the Flow-py model with the back-calculation plugin as used by the avalanche process in GR4A; HS = snow depth, DEM = digital elevation model. b) Example back calculation for the avalanche process (dark red), with the maximum energy line heights plotted in the background to show full process paths/runout (blue, yellow and light red). Black are raster cells with infrastructure that are located in the process paths and, therefore, the direct paths from raster cell to raster cell are identified that are possible between infrastructure and the associated starting cells (Avalanche start).

1) The **forest plugin** estimates the effect a forest has on the hazard process (protective effect) in terms of energy reduction (reduction of velocity and runout distances) dependent on the "actual" forest structure (Figure 8)
2) The advantage of the forest plugin is that it is flexible and customizable based on the available forest information. That is, one may have only information of the spatial extend of the forest cover in contrast to more detailed information on forest type and/or forest density, e.g. in terms of canopy cover or stem density. The available forest information is combined in a pre-processing step, which creates the Forest Structure Index (FSI) as a raster file (see below). A range of data levels and resolutions can be applied when employing the Flow-py forest plugin, but uncertainties included in the results decrease with increasing information depth.

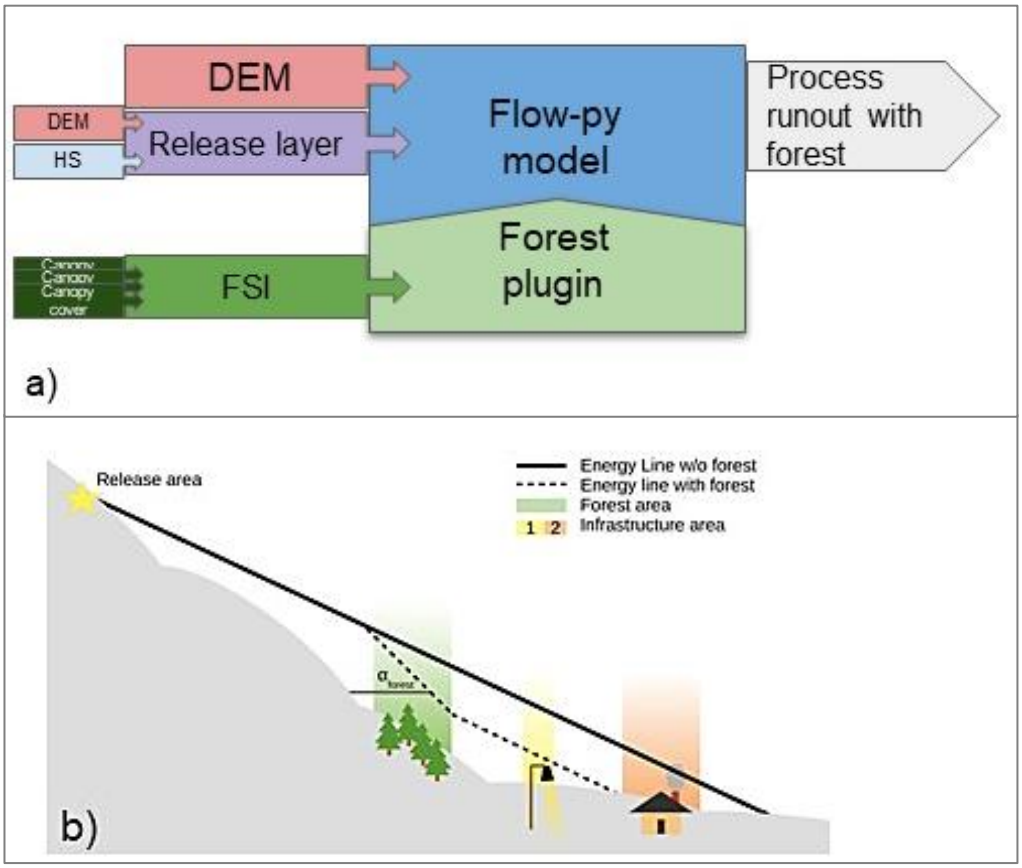

Figure 8: a) Workflow of the Flow-py model with the forest plugin as used by the avalanche process in GR4A; HS = snow depth, DEM = digital elevation model; FSI = Forest Structure Index. b) Forest plugin modelling principle, where α_{forest} is the increased runout angle α in forested areas, which depends on the FSI.

To keep the Flow-py forest plugin consistent with the philosophy of keeping input data simple and flexible with regards to data quantity and level the Forest Structure Index (FSI) has been introduced (Figure 8a). The FSI quantifies the structure of the forested area with regards to the forest's ability to impact the runout velocity and distance of a hazard process. The FSI ranges between 0 and 1, where 1 is the best forests with respect to natural hazard protection and 0 is a non-forested area. It should be noted that the best forest for natural hazard protection may be hazard specific, that

means that a highly effective protection forest for avalanches might not perform well with regards to rockfall protection. Three different levels of forest data can be employed to estimate the FSI and account for forest effects in the forest plugin of the Flow-py model.

- Level 1 data: Forest cover extent - forest yes/no
- Level 2 data: Forest type - default values are assigned to different types of forest
- Level 3 data: Forest structure/measurements – e.g. canopy cover, diameter at breast height (DBH) distribution, stem density, top height

As a minimum requirement level 1 data is needed to run the forest plugin, where a default value for the FSI is given to forested area, which should be between optimal hazard protection forest (FSI = 1) and shrubs and bushes (FSI = 0.2). Level 2 data can refine these default values to a more precise estimates and makes the forest across the landscape act in a more diverse manner. In GR4A, level 2 data is classified by tree species into forest types that are known to have an effect on avalanche and rockfall runout. To use level 3 data to calculate the FSI, the Maximum Forest Structure (MFS) value for each forest type is needed. Then the MFS is scaled with the level 3 data, which has been transformed into a utility score so different measurements can be compared and turned into a utility. The FSI is calculated by either adjusting and weighting the MFS with available level 3 data (Equation 1), or with a default density value of 0.8:

$$FSI = W1 \times Level\ 3\ data\ utility\ 1 \times MFS + W2 \times Level\ 3\ data\ utility\ 2 \times MFS$$

where Wi is a weight which gives preference to one utility over another.

In GR4A the forest data obtained for each of the PARs were available on different data levels, with some variability in the quality for each PAR. For all PARs, we were able to distinguish between different forest types (level 2 data), for some PARs level 3 data was also available. How these different data levels were applied or combined to retrieve the FSI is described for each PAR individually in D.T1.1.3.

The FSI is then used to adjust the α-angle (runout angle) of the hazard process in forested terrain as seen in Equation 2 (Figure 8b):

$$\alpha_{forest\_i} = \alpha + \left(FSI \times \alpha_{increase\_forest\_nh}\right)$$

where α_{forest_i} is the effective runout angle for the forested location i, and $\alpha_{increase\_forest\_nh}$ is the maximum increase to α in forested areas that is specific for a natural hazard process.

The effectiveness of the forest to slow a mass moving down a slope is co-determined by velocity. Therefore, we use the relationship between the empirical runout angle (α) model used in Flow-py and a similar model that can be derived from a very basic physical model assuming Coulomb friction since the empirical and the physical model result in the exact same equation. In Figure 6b, z_δ can be interpreted as the square of the velocity, assuming there is a non-zero mass. The increase to the runout angle in forested areas is reduced when the mass has high velocities. In modelling terms, the increase to the runout angle is scaled to the magnitude of z_δ. As the velocity dependent runout angle is different for rockfall and avalanches more details will be given in Sections 3.1.3 and 3.1.4.

Flow-py and the two plugins were applied to develop two map products as results of GR4A, and one spatial data set (the Impact Reduction Index) that is used as input data for the identification of exposure hotspots:

1. **Direct Object Protection Forest** is located between natural hazard release areas and endangered infrastructure (elements at risk).
   Developed for snow avalanches, rockfall and shallow landslides

2. **Efficient Green Mitigation Areas.** The map depicts highly effective areas for hazard energy reduction, suggesting potential afforestation areas for direct object protection forest, where no forest is growing at present, and existing direct object protection forest that is highly effective for hazard energy reduction.
   Developed for snow avalanches and rockfall

3. **Impact Reduction Index**. The Impact Reduction Index is defined for a specific location as the degree in which the surrounding "uphill" forest offers direct protection against a natural hazard process, decreasing the likelihood of that natural hazard reaching the location or decreasing its impact at this location. This data set is used as input data for the exposure hotspot analysis.
   Developed for snow avalanches and rockfall

The Direct Object Protection Forest and Efficient Green Mitigation Areas map products will be explained in more detail in D.T3.5.1. In Section 0, we explain how the Impact Reduction Index is retrieved.

3.1.2 Workflow: Landslides

The main aim of the spatial landslide analysis was to create a map that depicts areas where the present forest plays a role in reducing the (potential) impact of landslides. In this context, the expression impact relates to the area potentially affected by a landslide: it includes the initiation area of a landslide (release zone) and their likely downward paths (runout zone). Process impact areas are crucial to elaborate exposure hotspots (see section 3.2.3). This section describes how various model components were created and integrated to elaborate areas where present forests reduce the potential landslide impact in the six pilot action regions (PARs). In summary, the implemented approach included the analysis/modelling and integration of:

- Landslide **release susceptibility**: Areas prone to landslide release
- Landslide **process paths**: Areas affected by a landslide (release + path = impact area)
- Areas where the **current spatial forest distribution** plays a role in reducing landslide impact area

The availability of input data determines the applicability of spatially explicit landslide analysis techniques. In principle, spatial physically-based slope stability models are able to analyse the mechanical and hydrological (de)stabilizing effects of vegetation (Kuriakose et al., 2009; Schmaltz et al., 2019). However, the reasonable implementation of such models is usually restricted by the (un)availability of detailed spatial geotechnical, hydrological and geometric data (Seefelder et al.,

2017). A higher model flexibility (also in terms of input data) and high predictive performances are major advantages of using statistically-based spatial landslide models (Cascini, 2008; Frattini et al., 2010; Steger and Kofler, 2019). The complexity of a spatial model should be in balance with the input data quality (Corominas et al., 2013; Steger et al., 2017). The application of statistical/empirical approaches was considered the most suitable for GreenRisk4Alps after checking the available input data and the spatial extent of the PARs. Figure 9 highlights the main workflow behind the spatial landslide analysis.

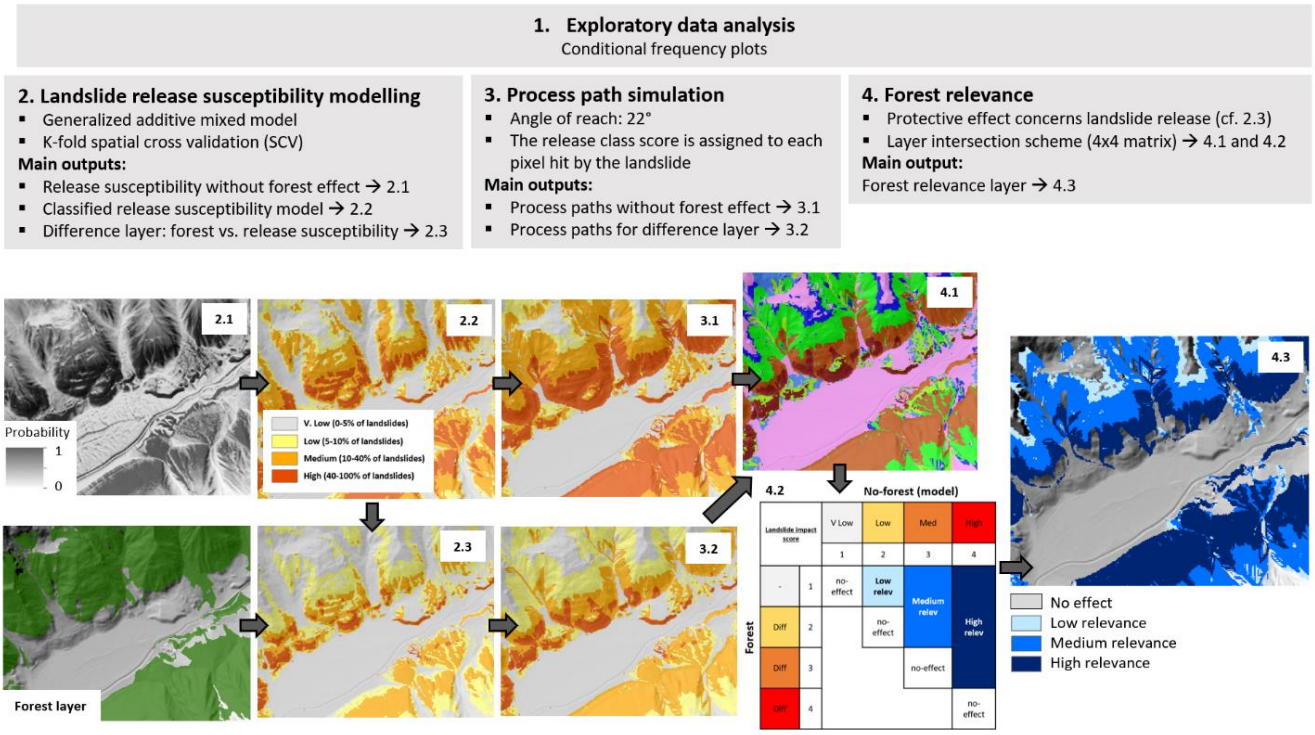

Figure 9: Overview of the implemented workflow steps for the spatially explicit landslide analysis. A dedicated landslide release susceptibility model was developed for the PARs Wipptal South and Vals/Gries. For the other PARs, landslide release probabilities (cf. 2.1) were estimated by a spatial transfer of prediction rules (only morphometry; details below).

Exploratory data analysis (step 1)

The exploratory data analysis was only conducted for the PARs Wipptal South and Vals/Gries, because for the other PARs consistent (shallow landslide) inventory data was not available. The exploratory data analysis was performed to gain insights into landslide inventory properties and to uncover potential data limitations. Empirical relationships between a variety of environmental variables (e.g. topography, land cover, geology) and the presence/absence of landslide occurrence were analyzed via conditional frequency plots (Steger et al., 2016). In summary, these plots visualize the conditional distribution of landslide presence/absence observations (e.g. binary variable) over continuous or categorical variables. Since the analysis was based on a 1:1 ratio of landslide presence to absence observations, a conditional frequency of > 0.5 relates to an overproportional density of landslides for the respective variable value (and vice versa).

Landslide release susceptibility modelling (step 2)

Landslide release susceptibility modelling was performed by building upon the principle 'the past is the key to the future'. A binary supervised classification algorithm (i.e. Generalized Additive

Model) was used to link past landslide locations (landslide release points mapped for Wipptal South and Vals/Gries) and landslide-absence locations with a variety of topographical and thematic features (e.g. slope angle, topographic wetness index, relative topographic position, aspect, landform variables, geology). Generalized Additive Model can account for non-linear relationships among landslide occurrence and multiple explanatory variables (Bordoni et al., 2020; J. N. Goetz et al., 2015; Petschko et al., 2014). In summary, the applied classifier allows to assess the environmental conditions which are typical for mapped landslides and those characteristic for stable locations. The derived statistical relationship can be used to spatially predict the likelihood of class-membership (e.g. class landslide presence) for each raster cell that contains information on the environmental variables. A predicted value close to 1 (see 2.1 in Figure 9) highlights that the observed environmental conditions are similar to the conditions observed at past landslide locations while a value close to 0 depicts typical stable conditions. More insights into principles behind data-driven landslide release susceptibility modelling can be found in Reichenbach et al. (2018), Steger (2017) and Steger and Kofler (2019).

The exploratory data analysis (step 1) and an associated literature review revealed that the available landslide information is heterogeneously complete among the land cover units. Thus, forest or land cover variables were not included as (fixed effect) variables in the final model to avoid an associated bias propagation (cf. Steger et al., 2017).
For instance, the observed high landslide densities in forested terrain for the PAR Wipptal South reflect the underlying data collection procedure (only damage causing landslides are inventoried) and not the “true” effect of forest. The high landslide densities in forested terrain can rather be explained by the high density of forest roads in the PAR and the systematic mapping of landslides that caused damage to these roads (Steger et al., 2020). The low landslide density in forests for the PAR Vals/Gries were also judged to depict a data bias, since the underlying mapping was based on orthophoto-interpretation. Previous research has shown that more than 50% of landslides (particularly shallow landslides) remain undetected under the forest canopy if the mapping is conducted on the basis of optical aerial imagery (Brardinoni et al., 2003; Jacobs et al., 2016). Even though we did not consider forest information for the model predictions, we accounted for its potential confounding effects by introducing land cover a random intercept as described in Steger et al. (2017). The validation of the release susceptibility models was based on the area under the receiver operating characteristics (AUROC) and a repeated non-spatial (cross validation; CV) and spatial (spatial cross validation; SCV) splitting of the original data into disjoint subsamples (training vs. test data) (Brenning, 2012).
Site-specific landslide release susceptibility models could not be trained for the PARs with unavailability of sufficient and consistent (shallow landslide) inventory data (Val Ferret, Oberammergau, Parc de Baronnies, Kranjska Gora). In order to get (basic) insights into landslide release susceptibility, a spatial transfer of the prediction rules was implemented. The underlying models were trained with available landslide information (Wipptal South and Vals/Gries) and by focusing only on topographic indices (e.g. slope angle, wetness index, topographic position, convergency). Care was taken to not transfer site specific particularities observed for the training regions (e.g. aspect in case of Vals/Gries). Iterative model adjustments (e.g. selection of variables, changing the flexibility of modelled relationships) were implemented by repeatedly comparing the derived spatial prediction pattern with the local morphology (hill shades) and visible erosion/landslide features (orthophoto).

Finally, all raw spatial prediction patterns (probabilities between 0 and 1; 2.1 in Figure 9) were classified into four classes by considering the portion of observed past landslides in the area (Wipptal South, Vals/Gries, cf. 2.2 in Figure 9) or by applying natural break classification that aims to minimize variation within each class while maximizing variation among the classes.

Process path simulation (step 3)

The aim of this step was to elaborate typical landslide process paths by simultaneously considering the respective landslide release zones (step 2). In simple terms, the landslide release classes were defined as starting zones and routed downslope according a typical landslide parameterization. In case of spatial overlaps (e.g. process paths of the class medium and high overlap), the highest release class score was assigned to each raster cell hit by the landslide. The BFW model Flow-py (see Section 3.1.1), which is an empirically based runout model, was used while an angle of reach of 22° was applied according previous analyses (GRAVIMOD II, Perzl et al. 2017). The process path classes were not only calculated for the landslide release model (2.2 in Figure 9), but also for the "difference layer" (2.3 in Figure 9) which accounts for the presence of forest (cf. step 4).

Forest effect (step 4)

A direct spatially explicit quantification of the forest protective effect was considered impracticable for the PARs, also because of missing spatial data and because the underlying landslide data underrepresents (Vals/Gries) or overrepresents (Wipptal South) landslides in forested terrain. Also a direct adaptation of previous research results (e.g. published values or functions that depict specific "stabilizing effects") was considered inappropriate, because many hydrological (e.g. evapotranspiration, canopy interception, water extraction from soil) and mechanical (e.g. surcharge, cohesion) effects of trees are site specific and change in space and time (Ghestem et al., 2011; Moos et al., 2016; Schmaltz et al., 2019; Sidle and Ochiai, 2006). For example, an elaboration of the mechanical effects of roots (i.e. root reinforcement) might require area-wide information on potential slip surface depths, because anchoring becomes particularly relevant as soon as the roots penetrate the sliding plane. At the same time, sliding surface might not be equally distributed in space and be co-determined by prevalent soil depths and topography (e.g. slope angles). Further spatial information on species distribution, age and soil properties might be necessary to approximate root distribution (penetration depth) while geotechnical soil parameters are also known to influence the cohesion forces of a plant. In summary, to render the task feasible in the context of GreenRisk4Alps, we build upon the literature-supported assumption that stabilizing effects of trees usually outweigh destabilizing effects for shallow landslide processes (e.g. Bathurst et al., 2010; Crozier, 1989; Goetz et al., 2015; Schmaltz et al., 2019, 2017; Sidle and Ochiai, 2006). Furthermore, we assumed that a forest located on a landslide-prone slope is more "relevant" compared to a forest on unsusceptible terrain (e.g. flat terrain or too steep terrain). The protective effect was considered at the level of the classified landslide release susceptibility model by intersecting the forest cover information to derive an initial "difference layer" (2.3 in Figure 9). This layer allowed to identify whether the respective release class is located in a forest or on non-forested terrain. It is important to note that the underlying one-class reduction for forested terrain can be considered a workaround to derive the necessary class-difference layer. After simulating process paths on the basis of both release maps (2.2 vs. 2.3 in Figure 9), a new combination layer (4.1 in Figure 9) was created on the basis of a 4x4 classification matrix (4 classes for each process path model; 4.2 in Figure 9). This procedure allowed to identify areas where the

protective effect of forest is relevant. Figure 10 exemplifies the principle behind the forest relevance layer.

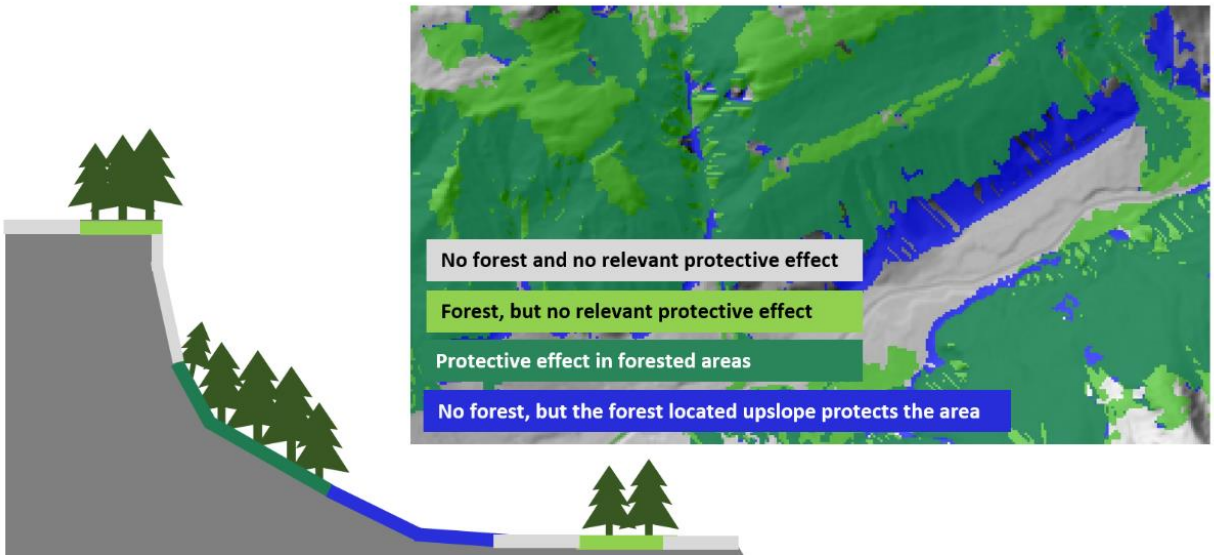

Figure 10: Principle behind the forest relevance layer for landslide processes. The light grey color (hillshade in the map) shows areas where forest is absent and where its protective effect plays no role (e.g. very low landslide release probability while the area cannot be reached by an uphill landslide). The light green areas are not relevant in terms of reducing landslide impact (same as grey area, but with forest cover). The dark green area shows forested terrain with a protective effect (e.g. the topographic conditions favour landslide release). The blue zones are not forested, but the upslope lying forest has a protective effect. Note that the final forest relevance layer further differentiates between a low, medium and high forest relevance (Figure 11)

Details to the original one-class forest relevance layer were added by examining the class of associated landslide impact zone (low, medium, high in 3.1 of Figure 9). We assigned a high relevance to an area in case the previously identified forest protective effect was associated with terrain conditions that exhibit a high likelihood of landslide impact. Thus, the three classes of the final map (Figure 11) highlight areas where forest plays a role in reducing the (potential) impact of landslides due to the direct presence of forest or due to forest that is located uphill. Among those three classes, the protective effect is considered more relevant if the general terrain conditions (e.g. morphology, lithology) favour a landslide impact. In simple terms, the area depicted in dark blue (high relevance) would be far more prone to a landslide impact if the forest (present at the location or uphill) is removed. A removal of forest in light blue areas (low relevance) might have less severe consequences in terms of landslide impact.

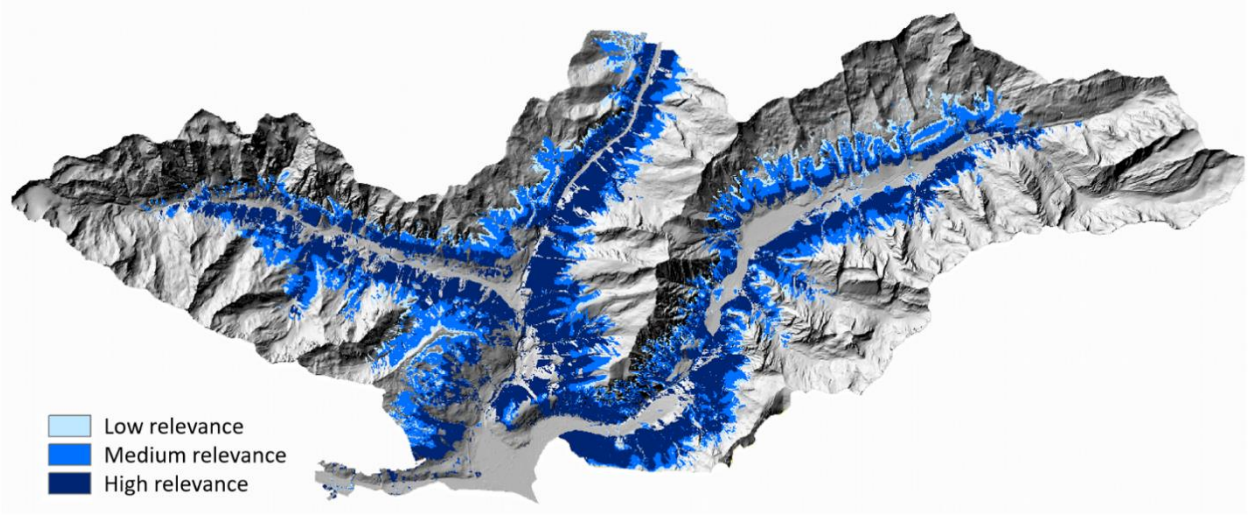

Figure 11: The landslide forest relevance layer exemplified for the PAR Wipptal South

3.1.3 Workflow: Avalanches

Identifying avalanche release areas (step 1)

We identified potential avalanche release areas following the approach from Perzl and Huber (2014). They used data from 1,432 recorded avalanche events to identify avalanche starting zones (according to the model of Perzl and Walter, 2012). Perzl and Huber (2014) developed a basic disposition model for avalanche release areas based on the ISDW evaluation matrix for the avalanche hazard potential (BMLFUW, 2008), and literature and empirical values. Two parameters were identified as key indicators for avalanche release probability that can be derived over large areas from DEMs:

- Snow depth (HS): An average of yearly maximum snow depths since avalanche release areas are more probable on slopes with deeper snow depths.
- Slope inclination: Mean slope inclinations ranging between 28° and 55° were found to be the inclination where the majority of avalanche starting areas occurs.

Reported slope inclination values for actual and potential avalanche release range between 10° and 60°; however, lower and upper range limits of 28° and 55° respectively are most often applied (Perzl and Huber, 2014). In the project the slope inclination was calculated from the 10-m DEM, which was also used as the input layer for the Flow-py model.

The mean maximum snow depth was calculated for each PAR by using several years of snow depth measurements from weather stations located inside the PARs or just outside the PAR boundaries. The weather stations' snow depth measurements and elevations were used to create a linear relationship between snow depth and elevation, which was used to approximate the mean maximum snow depth for each raster cell based on its elevation values. Therefore, the snow depth information is PAR specific.

Based on their explanatory data analysis, Perzl and Huber (2014) defined three limit values and limit functions (Figure 12), which we applied spatially to identify potential avalanche release areas for three release classes in every GR4A PAR:

- Class 1 (Anbruchklasse 1): mean maximum HS ≥ 50 cm (rare, avalanche danger level 4-5)
- Class 2 (Anbruchklasse 2): mean maximum HS ≥ 80 cm (frequent, avalanche danger level 2-5)
- Class 3 (Anbruchklasse 3): mean maximum HS ≥ 171 cm (very frequent, avalanche danger level 1-5)

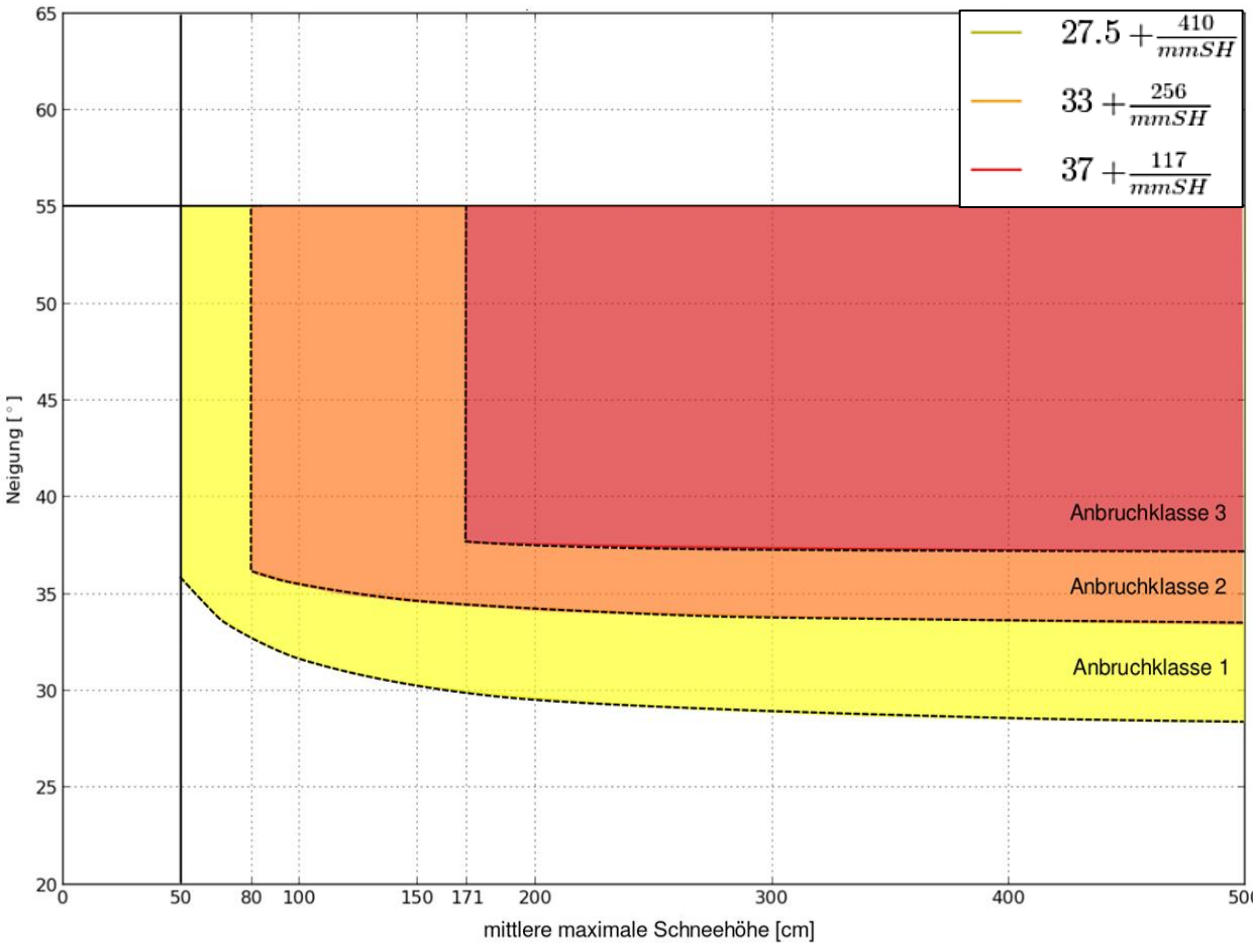

Figure 12: Limit values and limit functions of the disposition model from Perzl and Huber (2014) for three avalanche release classes (Anbruchklassen) based on slope inclination (Neigung) and mean maximum snow depth (mittlere maximale Schneehöhe), which were used in GR4A to identify potential avalanche release areas. Source: Huber et al. (2015)

Avalanche runout simulations (step 2)

Since Flow-py is an empirically based runout model, the types of avalanches that are simulated depend on the avalanche observations, which were used to derive the runout angle α (Huber et al. 2017). In general, avalanche observations are mainly focused on large dry snow slab avalanches (avalanche size 3-5, large to extremely large avalanches according to EAWS standards, https://www.avalanches.org/standards/avalanche-size/), which are likely to damage infrastructure in the valley bottom. Huber et al. (2017) found a mean α-angle of 25° for 89

documented large avalanche events in Austria, which was applied to model avalanche runout with Flow-py for every GR4A PAR.

Modeling forest effects on avalanches with Flow-py and the forest plugin (step 3)

Forests growing in avalanche terrain are able to reduce the probability of slab avalanche formation and release (Schneebeli and Bebi, 2004), and runout distances of small to medium size avalanches that are released in forest gaps or slightly above the tree line without significant forest damage (Teich et al., 2012a); however, also for larger avalanches forests are still able to dissipate some energy from the flowing avalanche by breaking, uprooting and overturning the trees in the avalanche path as well as by woody debris entrainment (Takeuchi et al., 2018; Teich et. al, 2012a; Bartelt and Stöckli, 2001), but this effect is often marginal and can result in a higher destructive potential due to trees that are transported downhill in the avalanche debris. Therefore, forest cover extent and forest structure in terms of canopy cover, stem density, species composition and size and distribution of forest gaps directly influence the activity, i.e. frequency and intensity of avalanches in forested terrain (Bebi et al., 2009; Teich et al., 2014; see D.T1.3.2 for more information). The main protective effect of forest against avalanches is on avalanche release. For previously released avalanches, the secondary protective effect of forests on avalanche runout becomes relevant, i.e. mass reduction by snow detrainment, deceleration and even stopping (Bartelt and Stöckli, 2001; Anderson and McClung, 2012; Feistl et al., 2014). Within the first 100-200 m of an avalanche path, evergreen forests with a high stem density and dense canopy cover can significantly reduce runout distances of small to medium size avalanches (Teich et al., 2012a). To account for forest's protective effects against snow avalanches, we developed a method staying consistent with the regional scale modeling principal that we adopted for the Flow-py model of light flexible input data with regards to data quantity and level. That is, we use the state-of-the-art methods described in literature with the forest plugin, which addresses both effects of forest on avalanches: the reduction of avalanche release probability and the increased energy dissipation. The increased dissipation of energy is accomplished by increasing the friction angle dependent on the forest structure index (FSI) and the avalanches velocity (z_δ), which are introduced in section 3.1.1.

The updated equation specific to avalanches is shown below, which is used to adjust the runout angle ($\alpha_{avalanche}$) for the avalanche process due to forest (Equation 3):

$$\alpha_{avalanche\_forest\_i} = \alpha_{avalanche} + \left(FSI_{avalanche} \times \alpha_{increase\_forest\_avalanche}\right)$$

where $\alpha_{avalanche\_forest\_i}$ is the runout angle for the forest that is located at raster cell i (before scaling the runout with velocity, i.e. velocity = 0), $\alpha_{avalanche}$ = 25° which is our base non-forested runout angle, and the maximum runout angle increase due to forest is $\alpha_{increase\_avalanche\_forest}$ = 10° for the avalanche hazard.

The $\alpha_{avalanche\_forest\_i}$ must then be adjusted to the velocity of the avalanche. However, it is important to note that one forested location (raster cell) may be in the path of many avalanches that can have different velocities at the forested location. Therefore, the same forest can have a strong energy dissipation effect on some slower avalanches, where other avalanches might have a higher velocity when passing the forested location with a limited energy dissipation effect of that forest.
Figure 13 shows the relationship of z_δ, the avalanches velocity (in red) and the effective runout angle (including the FSI increase due to forest). At z_δ = 45 m (or velocity ~30 m/s) the forest is no

longer capable of reducing the avalanches energy according to Feistl et al. (2015) and Takeuchi et al. (2018), which is reflected in the forest plugin.

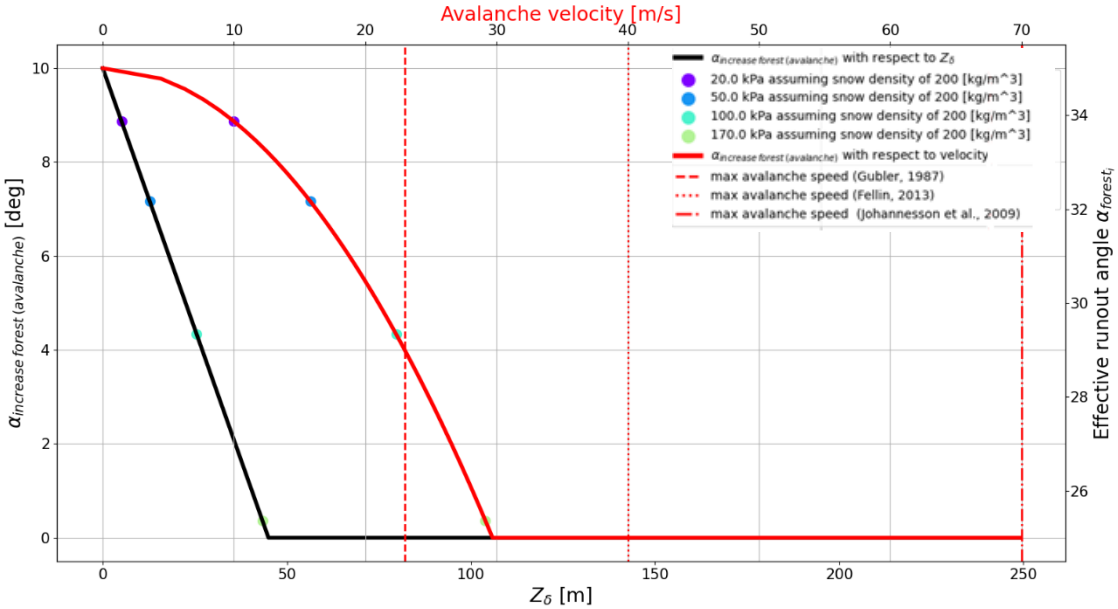

Figure 13: Relationship between z_δ (lower x-axis, black line), the increase to the α-angle in forested areas (left y-axis), the effective runout angle including the increase due to forest (right y-axis), and avalanche velocity (upper x-axis, red lines). That is, studies have found effects of forest on velocity, which can be linked to z_δ and, therefore, to $\alpha_{avalanche\_forest\_i}$

This value is reasonable when compared to the Swiss classification according to avalanche impact pressures and potential damages (Figure 14; Rapin, 2002). At 30 m/s an avalanche with a snow density of 200 kg/m³ would have a 170 kPa impact pressure, which is a larger impact pressure than is needed to destroy large forest areas and uproot large evergreen conifer trees. There is a limit imposed at z_δ = 250 m or at a velocity of ~ 70 m/s based on Johannesson et al. (2009).

Impact pressure (kPa)	Avalanche type	Potential damages
1-3	Powder snow/ Aerosol	Destroys a lonely tree (without forest protection)
1-4		Breaks the windows
>5-10		Destroys the forest
3-6	Dense snow	Pushes the gates, brooks/ crushes walls, roofs
3		Turnaround of a freight car (18 t)
8.5		Turnaround of a locomotive (120 t)
10		Serious damage of timber structures
20-30		Destroys timber structures, breaks the trees
50-100		Destroys a well developed forest
100		Pulling out large fir trees
>300		Movement of large blocks
1000		Movement of the reinforced concrete structures

Figure 14: Swiss classification according to impact pressures and potential damages. Source: Rapin (2002)

The following criteria were used in GR4A to rank different forest types (tree species composition) and forest structure parameters that in turn lead to the Forest Structure Index (FSI) score:

Level 1 data:

Level 1 data was available for every PAR, i.e. information about the location of forest.

Level 2 data:

Information about dominant tree species were available for every PAR, which was used to classify three forest types. The types are "evergreen coniferous forest", "deciduous and mixed forest"

(including larch-dominated forest), and "krummholz, bushes and shrubs". Some of the tree species that compose the forest types varied dependent on available data sets and institutions that collected the data. If no level 3 data was available for a PAR, default FSI-values ($FSI_{avalanche}$) were assigned to the forest types as shown in Table 4.

Table 4. Forest types (level 2 data) defined to quantify forest's protective effects on snow avalanches and respective Maximum Forest Structure ($MFS_{avalanche}$) and default Forest Structure Index ($FSI_{avalanche}$) values.

Forest type	Evergreen coniferous forest	Deciduous and mixed forest	Krummholz, bushes and shrubs
$MFS_{avalanche}$[a]	1	0.8	0.2
$FSI_{avalanche}$[a,b]	0.8	0.5	0.2

[a]For justification for forest type specific $FSI_{avalanche}$ scores and the $MFS_{avalanche}$ limits see Bebi et al. (2009), Teich et al. (2014) and Feistl et al. (2014); however, we do not use the exact reported values but rather the ranking of different forest types as well as forest densities (see also level 3 data).

[b]Default FSI-values were applied, if no level 3 data (forest structure information) was available.

Level 3 data:

For some PARs, spatial data on parameters characterizing forest structure was available. We used canopy cover expressed in a percentage and converted the measurement into a utility score between 0 and 1 as seen in Figure 15.

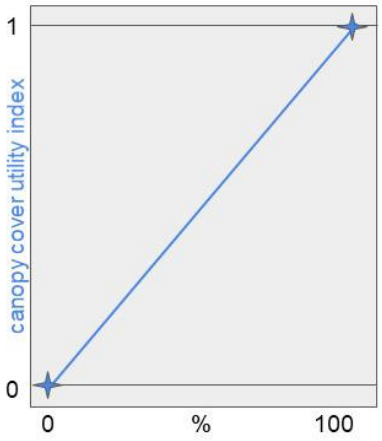

Figure 15: Canopy cover utility index that was developed for level 3 data to model forest effects on snow avalanches with Flow-py and the forest plugin (see Section 3.1.1 and Eq. 4).

The $FSI_{avalanche}$ was calculated for each forested raster cell from the canopy cover utility index and the $MFS_{avalanche}$-values (described in level 2 data) as seen in Equation 4:

$$FSI_{avalanche} = canopy\ cover\ utility\ index \times MFS_{avalanche}$$

The reduction in release probability that is embedded in the forest plugin is a result of adapting the forested runout angle based on forest structure ($FSI_{avalanche}$). If an avalanche starting cell is identified in forested terrain, the increase in runout angle due to the forest can stop the propagation of the avalanche before it starts. By definition the avalanche start cell will have a $z_\delta = 0$ and thus a velocity of 0. Therefore, the effective runout angle for the start cell (only for the avalanche associated with the start cell) will have values of (Equation 5):

$$\alpha_{avalanche\_forest\_i} = \alpha_{avalanche} + \left(FSI_{avalanche} \times \alpha_{increase\_forest\_avalanche}\right)$$

Hence an evergreen forest of highly effective structure with regards to avalanche energy dissipation ($FSI_{avalanche} = 1$) can nullify potential avalanche release areas starting on slopes of ≤ 35°, while forest with lesser capability of adjusting the runout angle ($FSI_{avalanche} < 1$) can stop avalanches from starting on slopes < 35°. Avalanche release areas >35° are not capable of being changed with the forest plugin, i.e. an avalanche will start despite the existence of forest. This is consistent with findings that avalanches can still release in and flow through forest on steep terrain (Bebi et al., 2009; Teich et al. 2012b). The mechanism for changing the runout angle in the avalanche path is the same as for changing the release model. For forested terrain the runout angle is increased due

to the forest with a maximum increase from 25° to 35° for well-developed dense evergreen forest to account for increased energy dissipation.

Calculation of the Impact Reduction Index (step 4)

The Impact Reduction Index (IRI) is an intermediate result produced by post-processing the Flow-py outputs to quantify the protective effects of forest on avalanche release and runout for a specific location. The IRI is the input data to the spatial analysis of the exposure hotspots model described in Section 3.2.3. For each PAR specific set of results, three Flow-py simulation runs were realized (Figure *16*): 1) a normal Flow-py simulation without any plugin, 2) accounting for forest effects on avalanche release and runout with Flow-py and the forest plugin, and 3) accounting for infrastructure in the avalanche path with Flow-py and the back-calculation plugin. For the avalanche hazard a set of results were produced separately for the three different release classes, resulting in a total of nine simulation runs for each PAR. The simulations along with the relevant output layers, which are raster files in the .tiff format, are:

- Flow-py (no plugin)
  - Cell counts: Number of starting cells that are tracked through a cell
  - Max z_δ: Maximum value of z_δ for every cell
  - Sum z_δ: Sum of all z_δ-values that track through a cell
- Flow-py with forest plugin
  - Sum z_δ: Sum of all z_δ-values that track through a cell
- Flow-py with back-calculation plugin
  - Back calculation: Shows every path that was taken from a start cell to an infrastructure cell

That is, a single raster pixel of the output layers can be located in the process paths of numerous avalanches that originate from different starting cells. Therefore, the high protective effect a forest has on a particular path against smaller avalanches (Teich et al., 2012a), is negligible to not present for the largest avalanches that could also occur on that path (Takeuchi et al., 2018). Therefore, it is critical to account for this avalanche size-dependent protective capacity of forest when calculating the IRI. We chose to base the IRI on the change of average z_δ. That is, the IRI is the differences in average z_δ between the Flow-py (no plugin) and the Flow-py with forest plugin simulations where z_δ can be interpreted as the energy of the avalanche. Therefore, the average z_δ is the average energy of all avalanches that pass through a particular raster cell.
The average z_δ is calculated by dividing the Sum z_δ by the Cell counts, which is the number of avalanches that track through a particular raster cell. We only use the cell counts for the non-forested case because avalanches that no longer reach a raster cell due to the increased energy dissipation by forest have a z_δ of 0.

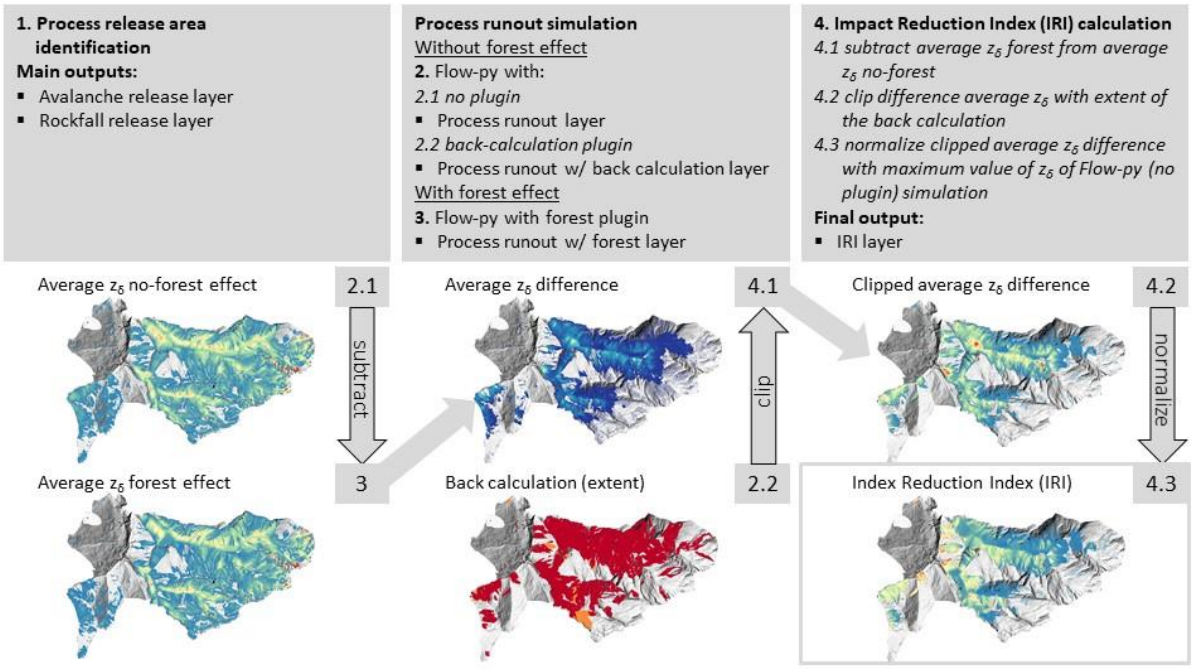

Figure 16: Overview of the workflow to calculate the Impact Reduction Index (IRI) for the natural hazard processes avalanches and rockfall exemplified for avalanches for the PAR Vals/Gries; z_δ = energy line height (ELH), which can be interpreted as the square of the velocity, assuming there is a non-zero mass. For a general overview of the Flow-py model, and the forest and back-calculation plugins see Section 0. For specific information on avalanches and rockfall see Sections 0 and 0

In Figure 16 the "average z_δ forest" was subtracted from the "average z_δ no-forest effect" Flow-py simulation output layer resulting in the difference in average z_δ. The back calculation highlights any pixel that was associated with an avalanche path that endangers infrastructure. We use the extent (highlighted areas) of the back calculation to clip the average z_δ difference resulting in the clipped average z_δ difference layer, which is a layer that only shows the effect of direct object protection forests on avalanche release and runout. To retrieve the IRI the clipped average z_δ difference layer is then normalized with the Max z_δ of the Flow-py (no plugin) simulation result, which highlights the forest effect relative to the maximum energy that would be expected in that avalanche path. We include this normalization step since the unnormalized average z_δ-value can be difficult to interpret, because raster cells with low maximum energy (Max z_δ) are expected to have a smaller unnormalized difference in average z_δ than cells with high Max z_δ, even if the forests located at low Max z_δ cells are efficient at reducing the avalanche energy they are exposed to.

3.1.4. Workflow: Rockfall

Identifying rockfall release areas (step 1):

Determining rockfall release probability is rather complex and dependent on rock quality, slope morphology, bedrock types, fracturing, mechanical properties of the rock, frequency, structures, weathering, erosion, seismicity, microclimate and hydrogeology (Volkwein et al. 2011, D.T.1.1.1). Available input data for rockfall simulations vary from PAR to PAR. Therefore, for the regional simulation of the six GR4A PARs, the determination of rockfall release probabilities was simplified rather dramatically compared to state-of-the-art process-based path specific models. That is, potential release areas were defined as areas with a mean slope inclination of ≥ 45° based on

slope inclination values prone to rockfall release ranging between 32° and 50° as described in literature (Gsteiger, 1993; Mölk and Rieder, 2017). We assumed that forest does not influence rockfall release, but trees in the release area can have a negative or positive effect. For example, they can increase rockfall release probability by root pressure in joints and increased weathering effects (Jahn, 1988). Also snow breakage and windthrow of trees in release areas might increase the rockfall frequency and, therefore, forest has no protective effect in instable areas or rather increases rockfall release probability (Jaboyedoff et al., 2005). It has been suggested to remove unstable trees from the top of release areas (Frehner et al., 2007) and, therefore, an efficient forest management needs to document the development of tree growth also in higher altitudes, in order to act accordingly and remove trees on top of potential release areas with a slope inclination ≥ 45°. For the GR4A project the forest effect in release areas was not considered.

Rockfall runout simulation (step 2)

In GR4A we separate landslides into rock slope failures (rockfall; extremely rapid to slow slope failures in rock), slope deformation (slow to extremely slow creeping-style deformations in rock) and soil slope failures (shallow landslides; extremely rapid to slow failures in soil; for detailed definitions see D.T1.4.1). In this section we describe the workflow for modeling the hazard type rockfall with the Flow-py model and the forest plugin (see Section 3.1.1).

The reach probability or runout distance describes the probability of falling, bouncing rocks reaching certain locations in their trajectories on the slope (Volkwein et al., 2011). Flow-py uses a simple slope angle criterion trajectory model for the simulation of reach probabilities of released rocks describing the probability, with which a block will reach a specific location on the slope with a given intensity (defined by probability of reach and kinematic energy). The basic runout angles (α-angles) of rockfall trajectories where boulders still can bounce, roll and slide range between 51.2° and 28.5° with an approximate mean given in several publications of 32° (e.g. Toppe, 1987; Colas et al., 2018). If the slope angle reaches about 25° blocks come to a halt (Lingua et al., 2020). In GR4A we therefore used an α-angle of 32° for simulations without forest.

Rockfall velocities for big rock avalanches (Bergsturz, > 1 Mio m^3) with a certain volume can reach up to 50 m/s (Dorren and Seijmonsbergen, 2003), and rockfall velocities on non-forested slopes range between 5 and 30 m/s (Dorren et al., 2005; Glover et al., 2012, Lateltin et al., 1997). We therefore applied a maximum velocity for rockfall processes of 40 m/s (Dorren et al., 2007); boulder bounce heights are not considered in the Flow-py model.

Modeling forest effects on rockfall with Flow-py and the forest plugin (step 3)

The main protective effects of forests against rockfall occur in the transit and deposit zones. Single trees dissipate energy of a rockfall impact by local penetration of the rock into the tree stem, deformation of the stem, rotation or translation of the root or rebound of the rock. Various studies analyzed the energy reduction capacity of different tree species through winching tests, dynamic impact tests and in-situ rockfall experiments (e.g. Dorren and Berger, 2006; Stokes et al., 2005; Dorren et al., 2006; Bertrand et al., 2013). These studies indicated a strong relationship between stem diameter and maximum amount of block energy reduction. Broadleaves-dominated forests including conifer species that tolerate shade such as silver fir and Norway spruce reach higher stem densities and high basal areas and have been proven to be very effective (Dupire et al., 2016). In general, broadleaved trees are more resistant against rockfall impacts than coniferous trees

(Dorren et al., 2005, Stokes et al., 2005). Thus, the higher the proportion of broadleaved trees in mixed forest types, the higher is the reduction of the runout distances as well as of kinetic energy values of the falling blocks (Dorren et al. 2005). Stem density highly influences rockfall velocity and rebounding heights dependent on kinetic energy reduction caused by the rocks hitting trees (Dorren et al., 2005). For this reason, stem number per hectare is the main forest parameter, which determines the effectiveness of the protective function of a stand (Dupire et al., 2016). One protection forest management guideline indicates a minimum stand density of 400 trees/ha without considering block dimensions (Wasser and Frehner, 1996). The Swiss guideline NaiS (Nachhaltigkeit und Erfolgskontrolle im Schutzwald) suggests at least 200 trees/ha with a mean DBH > 36 cm in optimal conditions and less than 150 trees/ha for the worst conditions (Frehner et al., 2005). These guidelines also mention that distances between trees in the fall direction should be less than 20 m, because falling blocks reach their maximum speed within 40 m, if no impact occurs (Dorren et al., 2005). The influence of forest top height is the opposite to stem density, i.e. higher top heights were found to be linked to longer rockfall runouts (Scheidl et al., 2020). A forest that shows the highest effectiveness against rockfall is, therefore, characterized by a high stem density and a high percentage of broadleaved tree species. The high stem density increases energy dissipation of blocks and reduces velocities. The optimal forest stand to withstand a rockfall hazard in the Alpine Space is coppice forest with shrubs, a high stand density and an average top height, which can reduce the rockfall hazard by 20% (Scheidl et al., 2020).

The following data was used to determine the Forest Structure Index (FSI) for forest with a protective function against rockfall, which was applied to account for forest effects in Flow-py simulations with the forest plugin:

Level 1 data:
For every PAR, information about the location of forests was available, i.e. the forest cover extent.

Level 2 data:
Data on forest composition was available for every PAR, which was used to classify three forest types by main tree species: "coppice, broadleaved and mixed forest", "coniferous forest", and "bushes and shrubs". Default FSI-values ($FSI_{rockfall}$) were assigned to these forest types for PARs with only level 2 data (Table 5).

Table 5. Forest types (level 2 data) defined to quantify forest's protective effects on rockfall and respective Maximum Forest Structure ($MFS_{rockfall}$) and default Forest Structure Index ($FSI_{rockfall}$) values.

Forest type	Coppice, broadleaved and mixed forest	Coniferous forest	Bushes and shrubs
$MFS_{rockfall}$	1	0.8	0.2
$FSI_{rockfall}$[a]	0.8	0.64	0.2

[a]Default FSI-values were applied, if no level 3 data (forest structure information) was available.

Level 3 data:
For some PARs forest measurements were available. For these PARs, we assigned each of the forest types (level 2 data) a Maximum Forest Structure ($MFS_{rockfall}$) value based on their overall ability to reduce rockfall impact (Table 5). We then used stem density and top height, which were turned into utility indices as seen in Figure 17 to adjust the $MFS_{rockfall}$ in order to obtain the $FSI_{rockfall}$.

Before adjusting the $MFS_{rockfall}$, level 3 data is translated into utilities called stem number utility index and/or a top height utility index that we developed based on literature values (see Figure 17).

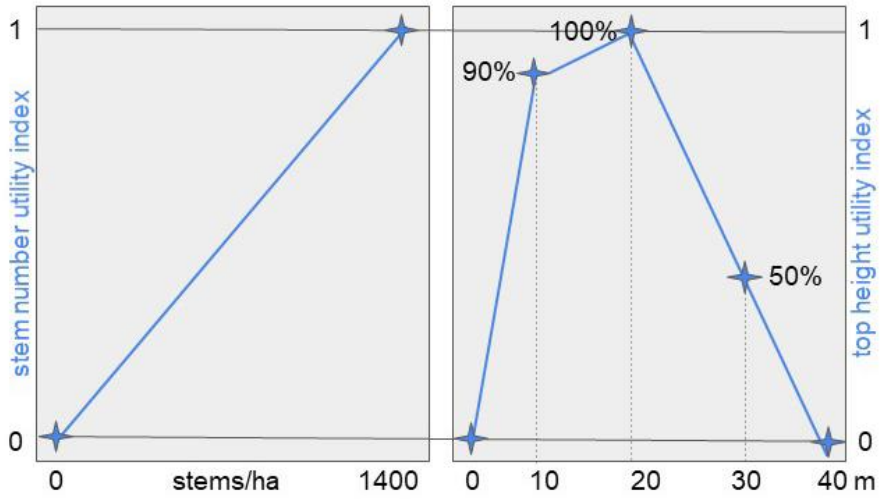

Figure 17: Stem number and top height utility indices that were developed for rockfall level 3 data to model forest effects with Flow-py and the forest plugin (see Section 0 and Eq. 6).

To determine the $FSI_{rockfall}$, the $MFS_{rockfall}$ were then adjusted and weighted with the utility indices (Equation 6):

$$FSI_{rockfall} = 0.5 \times stem\ number\ utility\ index \times MFS_{rockfall} + 0.5 \times top\ height\ utility\ index \times MFS_{rockfall}$$

The $FSI_{rockfall}$ is used to adjust the $\alpha_{rockfall}$-angle (runout angle) of the rockfall process in forested terrain (Equation 7):

$$\alpha_{rockfall\_forest\_i} = \alpha_{rockfall} + \left(FSI_{rockfall} \times \alpha_{increase\_forest\_rockfall}\right)$$

where $\alpha_{rockfall}$ is 32°, $\alpha_{rockfall\_forest\_i}$ is the effective runout angle for the forested location i, and the maximum increase to runout angle $\alpha_{increase\_rockfall\_forest}$ is 13° for the rockfall hazard in forested areas.

To determine the $\alpha_{increase\_rockfall\_forest}$, the $\alpha_{rockfall}$-angle was adjusted based on the relationship of z_δ and the rockfall velocity in forests as found in the literature (Figure 18). That is, forest has an effect on rockfall between velocities of 0 and 45 m/s. After that threshold, the effect of forest on rockfall runout is negligible.

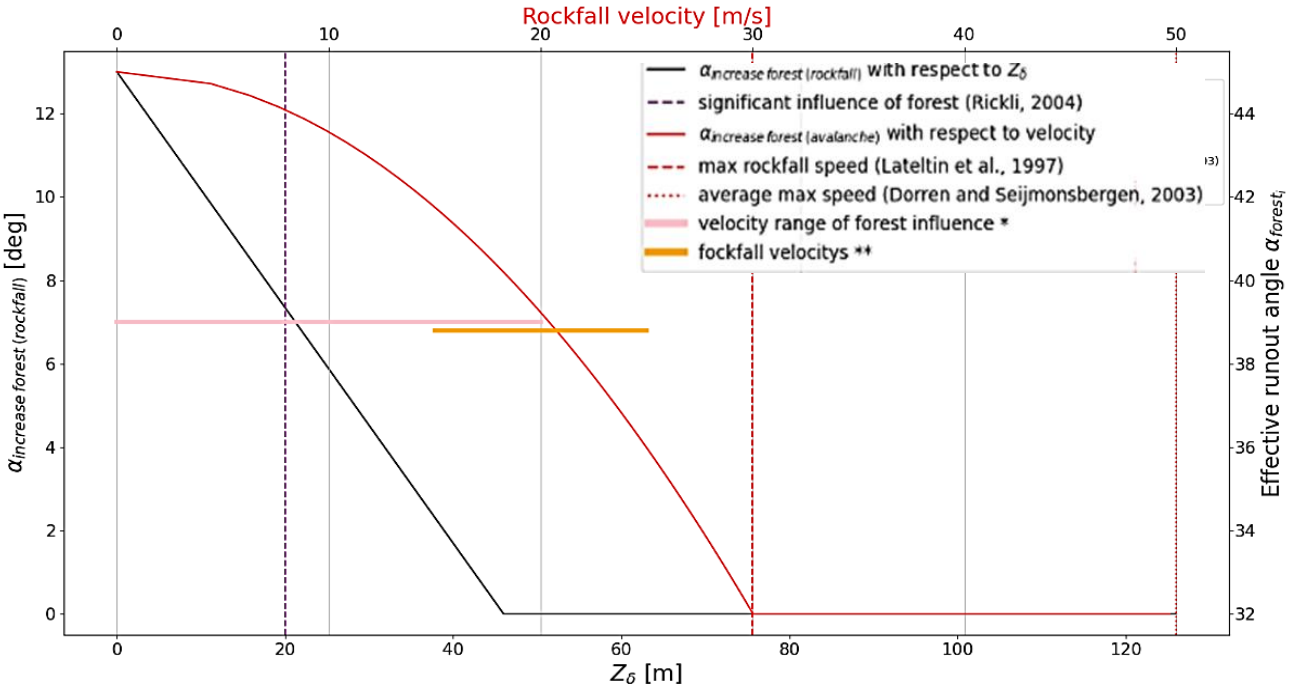

*Figure 18: Relationship between z_δ (lower x-axis, black line), the increase to the α-angle in forested areas (left y-axis), the effective runout angle including the increase due to forest (right y-axis), and rockfall velocity (upper x-axis, red lines). That is, studies have found effects of forest on velocity, which can be linked to z_δ and, therefore, to $\alpha_{increase\_rockfall\_forest}$. The pink and orange lines are velocity ranges where forest had been proven to have an effect (pink, *Rickli et al., 2004) or in forests measured rockfall velocities (orange, **Jahn, 1988; Zinggeler, 1990; Gsteiger, 1993; Doche, 1997; Dorren et al., 2004; Perret et al., 2004).*

In summary, we used the following thresholds to account for the protective effect of forests in rockfall transit zones in Flow-py with the forest plugin:

1. Increase of α-angle by a maximum of 13° in forested areas. Field experiments and simulations have shown a range of increase of the α-angle between 6° and 14° due to forest over the full path (Oswald, 2020; Dorren et al., 2005). We chose to use a value on the higher side of this spectrum, because the Flow-py model only applies the increase to runout angle to raster cells with forest. Furthermore, the 13° are scaled by the $MFS_{rockfall}$ to further reduce the effect that forest has on runout.
2. Since we assume an angle of 32° for the transit of rockfall events and release areas ≥ 45°, an $\alpha_{increase\_rockfall\_forest}$ of 13° is the maximum increase to the α-angle that can be applied before it would affect the model used to identify starting areas. This is because 32° + 13° = 45° and, therefore, an $\alpha_{increase\_rockfall\_forest}$ > 13° would meet the stopping criteria and stop the rock before it moved from the starting raster cell.

Calculation of the Impact Reduction Index (step 4)

The calculation of the rockfall Impact Reduction Index follows the same steps as describe for avalanches (see Section 3.1.3). Because the rockfall release model differs from the avalanche release model, i.e. it considers only one release class and not three, only three model runs in total were needed for rockfall simulations for each PAR in contrast to nine simulations for avalanches.

3.2. Exposed elements

As described in Chapter 1 of this report, exposure is, besides hazard and vulnerability, one of the three components determining the risk. Where chapter 2 describes the Rapid Risk Appraisal as a tool to measure the capability of a region to manage risks, which can be used as an indicator for the vulnerability of a region and chapter 3.1 documenting the calculation of the hazards considered in this project, this section deals with the exposure. Exposure, as defined by the IPCC, refers to "..the presence of people; livelihoods; environmental services and resources; infrastructure; or economic, social, or cultural assets in places that could be adversely affected" (IPCC, 2014). In the following sections we will describe in detail how we accounted for the exposure component to identify hotspots where forest has a high relevance in reducing the impact of gravitational hazards. The overarching question of this analysis was: Where does the presence of forest reduce the impact of gravitational natural hazards to potentially exposed buildings or transport and recreational infrastructure? The underlying objectives in order to answer this question were to

1) Identify those areas where hazard exposure is reduced due to the presence of forest in the GR4Alps Pilot Areas for the three hazards landslide, avalanche and rockfall
2) Rank the forest effect in reducing the hazard exposure by assessing the impact of each hazard type on different types of assets with and without forest effect
3) Spatially visualise those areas where the exposure reduction effect due to forest presence is greatest within a Pilot Area

Main results of this analysis will be annotated maps, datasets, a process description, and documentation of results. From the spatial hotspots coming out of the exposure analysis three hotspots within each Pilot Area will be selected for further use in the TEGRAV economic model (see also Figure 4 in DT 2.4.2).

3.2.1. Selection and classification of asset types

For this analysis, buildings, transport and recreational infrastructure were considered as exposed elements. Recreational infrastructure was included since in all Pilot Areas tourism and outdoor activities are of major importance and economic value. Deliverable 2.4.2 describes in detail the processes of selecting types of assets potentially exposed, the data collection process and data availabilities in each PAR and the categorisation of two priority classes of assets. It notes that the classification of assets into high and low priority follows the recommendations of Perzl et al. (Perzl, 2014). To summarise, the two priority classes for buildings is composed of residential, commercial and industrial buildings classified as high priority and all other buildings (e.g. garages, stables) classified as lower priority. It has to be noted that not for all Pilot Areas the available data allowed to make this distinction. In those cases where no distinction could be made all buildings were considered high priority. Regarding transport infrastructure assets such as motorways, primary and secondary roads were regarded high priority whereas tertiary roads, e.g. roads within settlements were categorised as low priority. Forest tracks were not included in the analysis. Recreational structures such as for instance cable cars, campsites, ski runs, golf courses or sports ground were considered assets of lower priority. Figure 19 shows an example of the different types of exposed elements in the area around the town of Vipiteno in the Pilot Area Wipptal South in Italy.

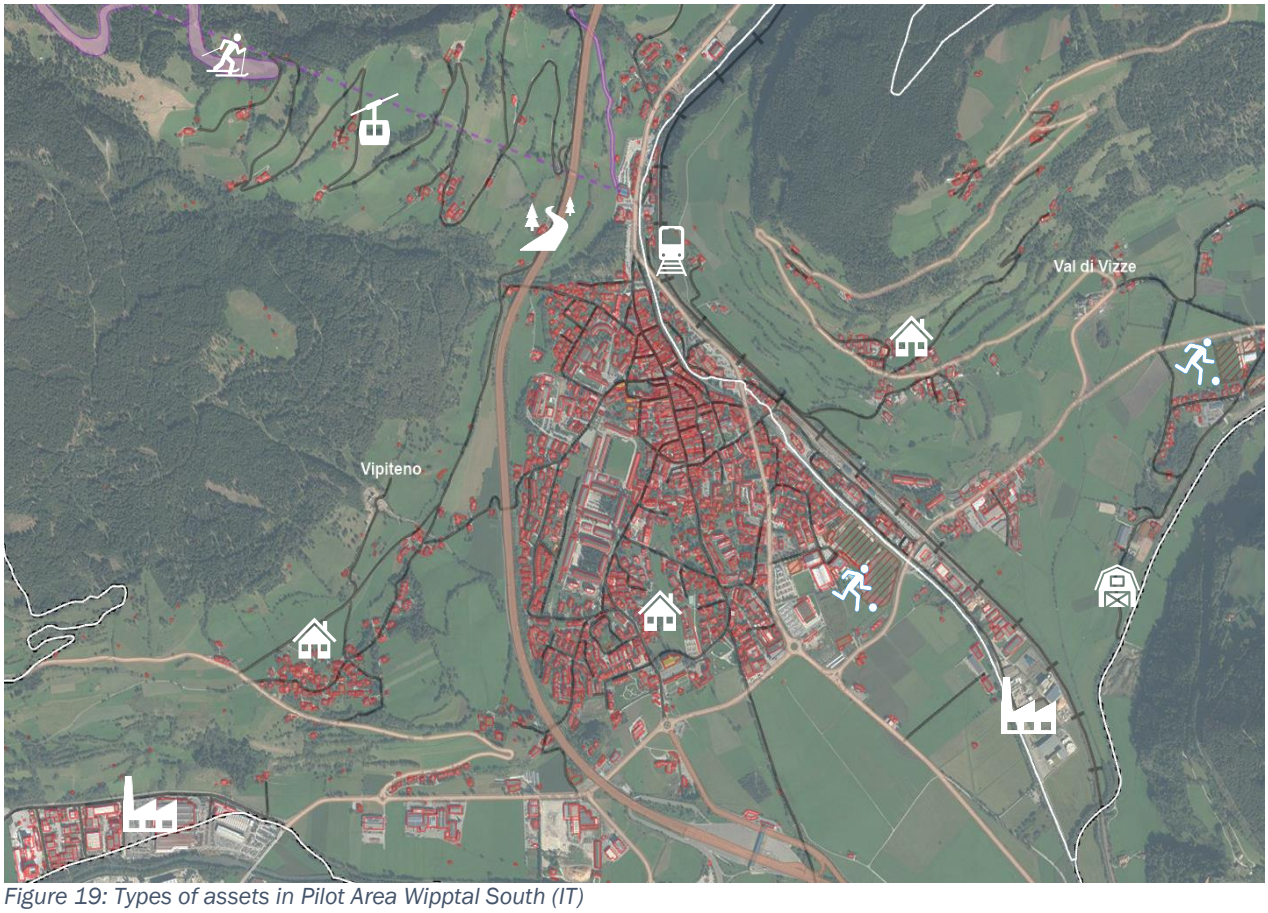

Figure 19: Types of assets in Pilot Area Wipptal South (IT)

Buildings and infrastructure remained separate types of assets in the processing and visualisations since consequences, such as potential systemic impacts, but also risk mitigation measures differ depending whether a building or a transport infrastructure or a recreational site are impacted.

Pre-processing of input data

The geospatial data needed for the exposure analysis were made available in different formats and different levels of detail (thematic and spatial) by the PARs. Data format in all cases was vector. In a first step buildings, transport and recreational features were extracted from the original data sets. In a second step the assets were attributed classes as defined and according to their value, i.e. high value = 2 and low value =1. All asset information was subsequently converted into 10m resolution raster data sets (Figure 20).

Figure 20: Rasterised asset information (buildings and road classes)

3.2.2. PAR assets maps and/or statistics

In order to spatially identify those areas where forest has a significant relevance in reducing the impact of gravitational hazards, hazard modelling results (for method and result description see chapter 3.1) were superimposed over the classified asset information. Building classes combined with forest relevance classes were visualised and areas per combined class quantified for the entire pilot region (Figure 21 and Figure 22)

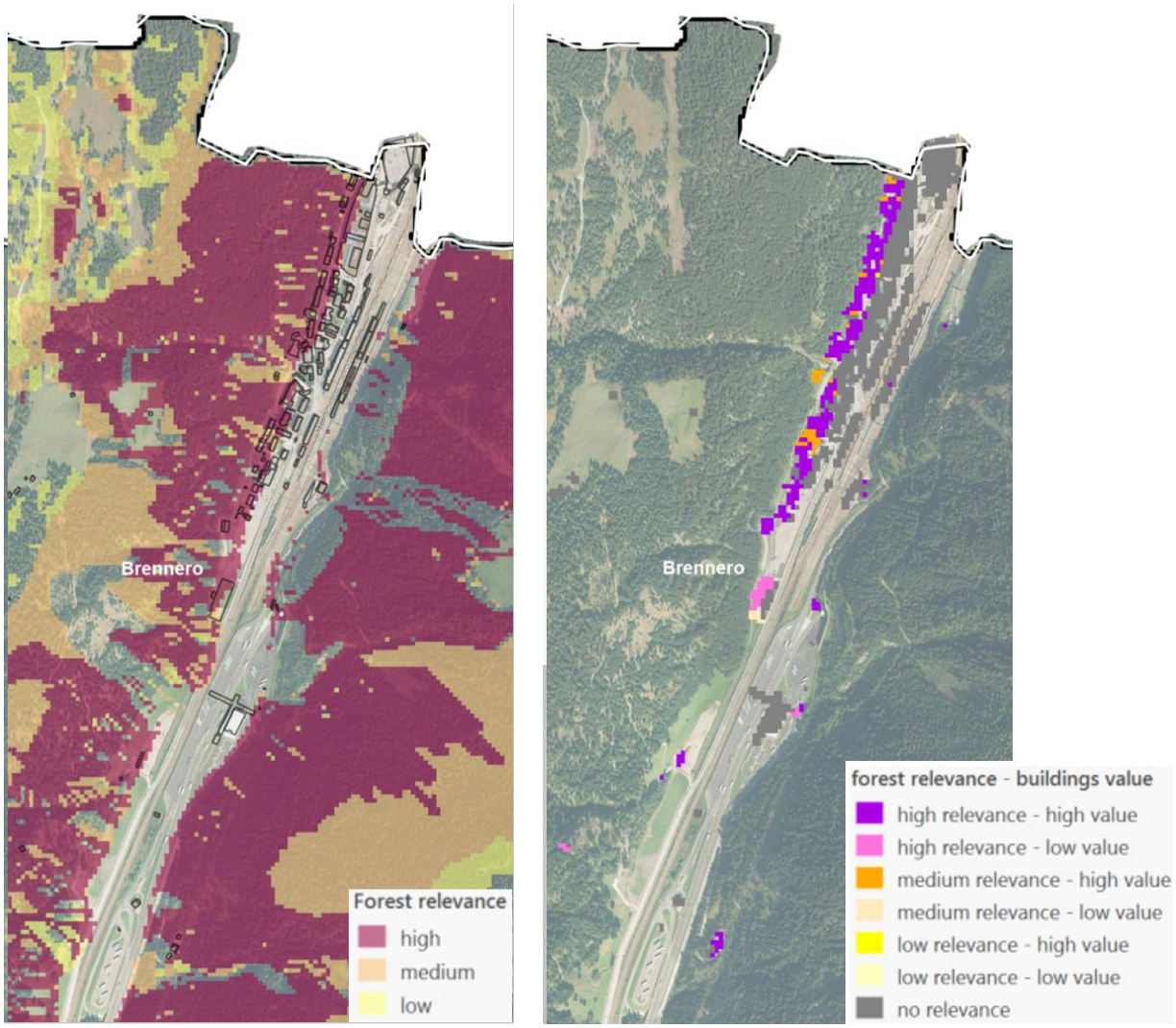

Figure 21: The map on the left shows the forest relevance in reducing the impact of landslides classified in three classes in the far north of the Pilot Area Wipptal South (IT). Building footprints are shown with black outlines. The map on the right shows the forest relevance classes combined with the building classes.

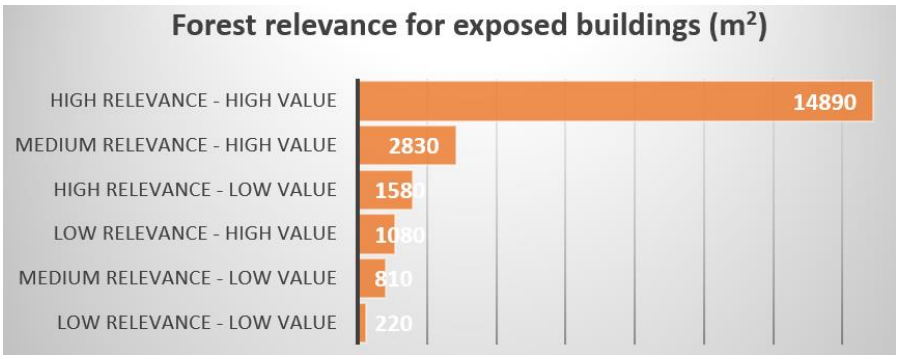

Figure 22: Quantification of area of building classes with a reduced impact from landslide hazards due to the presence of forest in the Pilot Area Wipptal South (IT)

The same procedure was followed for transport and recreational infrastructure (Figure 23 and Figure 24).

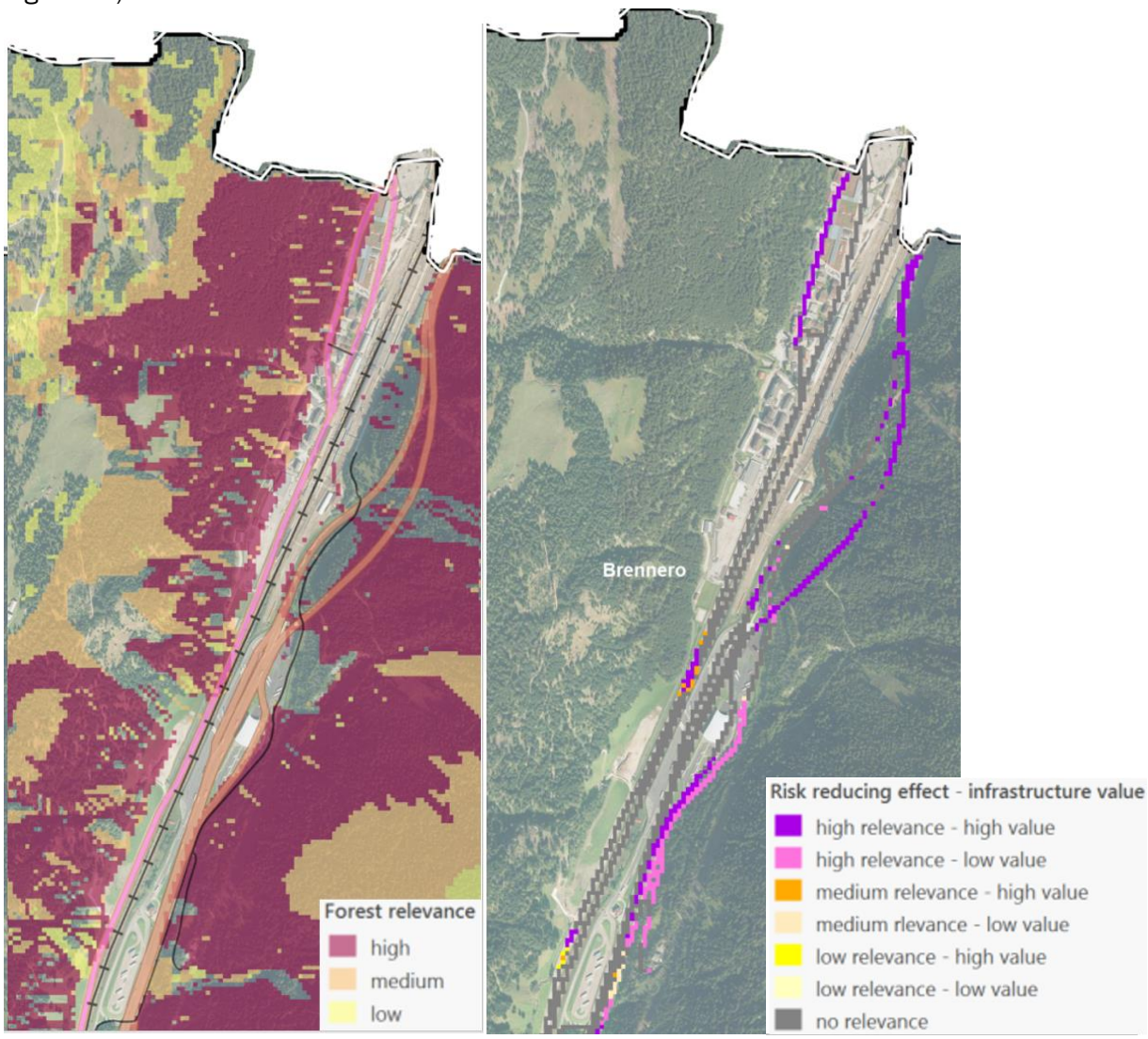

Figure 23: The map on the left shows the forest relevance in reducing the impact of landslides classified in three classes in the far north of the Pilot Area Wipptal South (IT). Transport infrastructure is shown as black lines. The map on the right shows the forest relevance classes combined with the transport infrastructure classes.

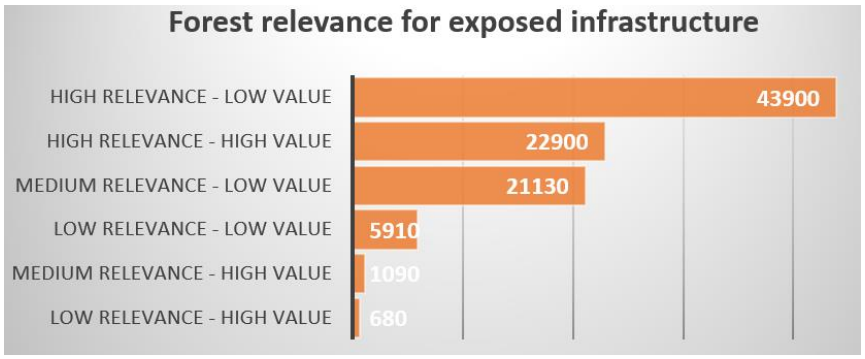

Figure 24: Quantification of area of transport infrastructure classes with a reduced impact from landslide hazards due to the presence of forest in the Pilot Area Wipptal South (IT)

3.2.3. Identifying exposure hotspots

The combined forest relevance-exposure maps developed in the previous step were used to identify few exposure hotspots. Quantitatively this was done by aggregating the high relevance/high value assets to larger features allowing a qualitative selection by local stakeholders (Figure 25 and Figure 26).

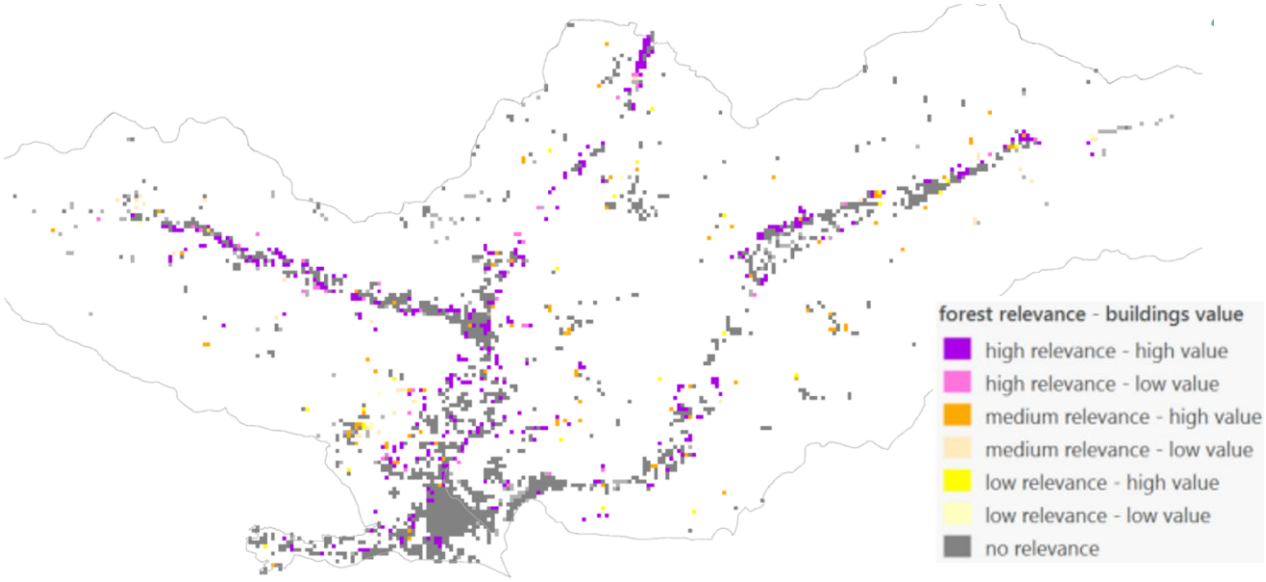

Figure 25: This map shows the Pilot Area Wipptal South (IT) and the high relevance/high value building sites

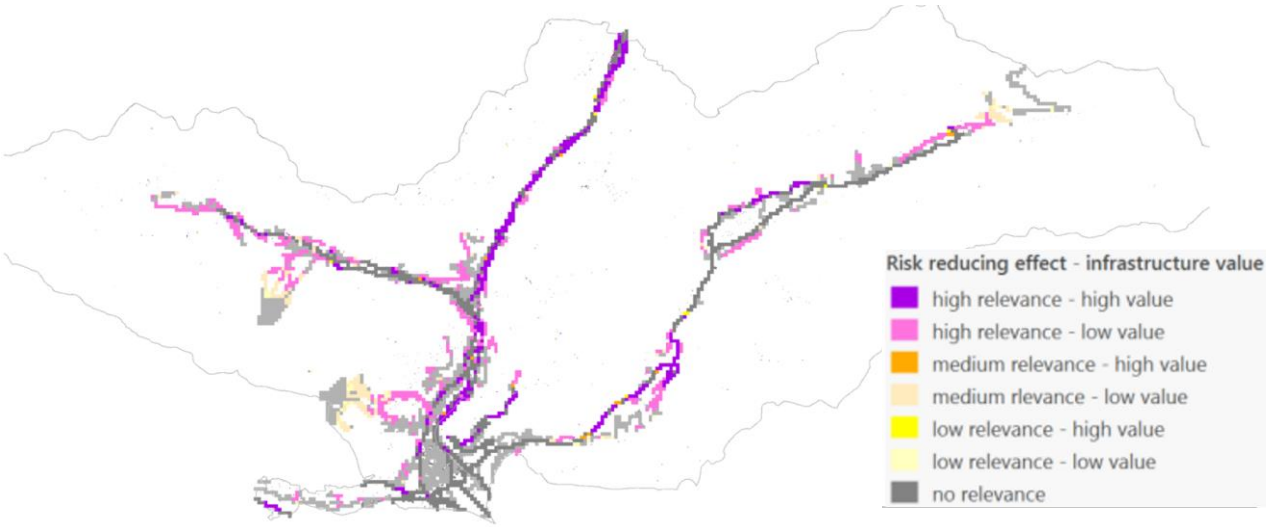

Figure 26: This map shows the Pilot Area Wipptal South (IT) and the high relevance/high value transport infrastructure sites

4. Outlook

The workflow described in this deliverable allows to identify the areas where the exposure reduction effect due to forest presence is greatest within each PAR. Within the project, these areas are referred to as “Exposure hotspots”. For each PAR, exposure hotspots are adopted to select relevant profiles on which to apply the TEGRAV economic model. TEGRAV aims to help decision makers choose among different risk mitigation measures, namely TEchnical, GReen and AVoidance measures. In particular, for each identified profile, an overview of the direct and indirect costs, avoided damages and benefits of the different considered measures will be provided. For more details on the TEGRAV model, refer to the deliverables D.T. 3.3.1 and 3.3.2. The results of the activities described in this deliverable and their integration with the TEGRAV are presented in D.T.3.5.1. Overall, analysing the risk management practices in place in the PARs and comparing costs and benefits of different measures, will allow to develop an innovative ecosystem-based risk management strategy, fulfilling the overall objective of the project.

5. References

Alcántara-Ayala, I., 2002. Geomorphology, Natural Hazards, Vulnerability and Prevention of Natural Disasters in Developing Countries. Geomorphology 47, 107–124. https://doi.org/10.1016/S0169-555X(02)00083-1

Anderson, G., McClung, D., 2012. Snow avalanche penetration into mature forest from timber-harvested terrain. Canadian Geotechnical Journal 49(4), 477-484.

Bartelt, P., Stöckli, V., 2001. The influence of tree and branch fracture, overturning and debris entrainment on snow avalanche flow. Annals of Glaciology 32, 209-216.

Bathurst, J.C., Bovolo, C.I., Cisneros, F., 2010. Modelling the effect of forest cover on shallow landslides at the river basin scale. Ecological Engineering 36, 317–327. https://doi.org/10.1016/j.ecoleng.2009.05.001

Bebi, P., Kulakowski, D., Rixen, C., 2009. Snow avalanche disturbances in forest ecosystems—State of research and implications for management. For. Ecol. Manage. 257, 1883–1892. https://doi.org/10.1016/j.foreco.2009.01.050.

Bertrand, D., Bourrier, F., Olmedo, I., Brun, M., Berger, F., Limam, A., 2013. Experimental and numerical dynamic analysis of a live tree stem impacted by a Charpy pendulum. International Journal of Solids and Structures, 50(10), 1689-1698.

BMLFUW, 2008. ISDW-Handbuch für Detailprojekte. Initiative Schutz durch Wald (ISDW). Bundesministerium für Land- und Forstwirtschaft, Umwelt- und Wasserwirtschaft (BMLFUW).

Bordoni, M., Galanti, Y., Bartelletti, C., Persichillo, M.G., Barsanti, M., Giannecchini, R., Avanzi, G.D., Cevasco, A., Brandolini, P., Galve, J.P., Meisina, C., 2020. The influence of the inventory on the determination of the rainfall-induced shallow landslides susceptibility using generalized additive models. CATENA 193, 104630. https://doi.org/10.1016/j.catena.2020.104630

Brardinoni, F., Slaymaker, O., Hassan, M.A., 2003. Landslide inventory in a rugged forested watershed: a comparison between air-photo and field survey data. Geomorphology 54, 179–196. https://doi.org/10.1016/S0169-555X(02)00355-0

Brenning, A., 2012. Spatial cross-validation and bootstrap for the assessment of prediction rules in remote sensing: The R package sperrorest, in: Geoscience and Remote Sensing Symposium (IGARSS), 2012 IEEE International. pp. 5372–5375.

Cardona, O.D., van Aalst, M.K., Birkmann, J., Fordham, M., McGregor, G., Perez, R., Pulwarty, R.S., 2012. Determinants of Risk: Exposure and Vulnerability, in: Field, C.B., Barros, V., Stocker, T.F., Qin, D., Dokken, D.J., Ebi, K.L., Mastrandrea, M.D., Mach, K.J., Plattner, G.-K., Allen, S.K., Tignor, M., Midgley, P.. (Eds.), Managing the Risks of Extreme Events and Disasters to Advance Climate Change Adaptation. Cambridge University Press, UK; New York, NY, USA, pp. 65-108.

Cascini, L., 2008. Applicability of landslide susceptibility and hazard zoning at different scales. Engineering Geology 102, 164–177. https://doi.org/10.1016/j.enggeo.2008.03.016

Colas, B., Berger, F., Toe, D., 2018. Run-out of rockfall: towards objective assistance in determining the angles of the energy line method. 4th Rock Slope Stability Symposium, Chambery.

Corominas, J., van Westen, C., Frattini, P., Cascini, L., Malet, J.-P., Fotopoulou, S., Catani, F., Van Den Eeckhaut, M., Mavrouli, O., Agliardi, F., Pitilakis, K., Winter, M.G., Pastor, M., Ferlisi, S., Tofani, V., Hervás, J., Smith, J.T., 2013. Recommendations for the quantitative analysis of landslide risk. Bulletin of Engineering Geology and the Environment. https://doi.org/10.1007/s10064-013-0538-8

Crozier, M.J., 1989. Landslides: causes, consequences & environment. Routledge, London; New York.

Cruden, D.M., Varnes, D.J., 1996. Landslide Types and Processes, TRB Special Report. National Academy Press, Washington.

Dorren, L. K. A., Berger, F., 2006. Stem breakage of trees and energy dissipation during rockfall impacts. Tree Physiol. 26, 63–71.

Dorren, L. K. A., Berger, F., Putters, U. S., 2006. Real-size experiments and 3-D simulation of rockfall on forested and non-forested slopes. Natural Hazards and Earth System Science, 6 (1), 145-153.

Dorren, L., Berger, F., Jonsson, M., Krautblatter, M., Mölk, M., Stoffel, M., Wehrli, A., 2007. State of the art in rockfall–forest interactions. Schweizerische Zeitschrift für Forstwesen, 158(6), 128-141.

Dorren, L.K., Berger, F., le Hir, C., Mermin, E., Tardif, P., 2005. Mechanisms, effects and management implications of rockfall in forests. Forest Ecology and Management, 215(1-3), 183-195.

Dorren, L.K., Seijmonsbergen, A.C., 2003. Comparison of three GIS-based models for predicting rockfall runout zones at a regional scale. Geomorphology, 56(1-2), 49-64.

Dupire, S., Bourrier, F., Monnet, J.-M., Bigot, S., Borgniet, L., Berger, F., Curt, T., 2016. The protective effect of forests against rockfalls across the French Alps: Influence of forest diversity. Forest Ecology and Management, 382, 269-279.

Federal Office for Civil Protection (FOCP), 2014. Integrated Risk Management. Its importance in protecting people and their livelihoods. Bern, Switzerland.

Feistl, T., Bebi, P., Christen, M., Margreth, S., Diefenbach, L., Bartelt, P., 2015. Forest damage and snow avalanche flow regime. Nat. Hazards Earth Syst. Sci. 15, 1275–1288.

Feistl, T., Bebi, P., Teich, M., Bühler, Y., Christen, M., Thuro, K., Bartelt, P., 2014. Observations and modeling of the braking effect of forests on small and medium avalanches. Journal of Glaciology 60(219), 124-138.

Frattini, P., Crosta, G., Carrara, A., 2010. Techniques for evaluating the performance of landslide susceptibility models. Engineering Geology 111, 62–72. https://doi.org/10.1016/j.enggeo.2009.12.004

Frehner, M., Wasser, B., Schwitter, R., 2005. Nachhaltigkeit und Erfolgskontrolle im Schutzwald. Wegleitung für Pflegemassnahmen in Wäldern mit Schutzfunktion. Bundesamt für Umwelt, Wald und Landschaft, Bern, 564.

Frehner, M., Wasser, B., Schwitter, R., 2007. Sustainability and Success Monitoring in Protection Forests: Guidelines for Silvicultural Interventions in Forests with Protective Functions. Federal Office for the Environment FOEN.

Gamma, P., 1999. dfwalk – Ein Murgang-Simulationsprogramm zur Gefahren-zonierung. PhD thesis, Universität Bern.

Ghestem, M., Sidle, R.C., Stokes, A., 2011. The influence of plant root systems on subsurface flow: implications for slope stability. BioScience 61, 869–879.

GIZ, EURAC, 2017. Risk Supplement to the Vulnerability Sourcebook. Guidance on how to apply the Vulnerability Sourcebook's approach with the new IPCC AR5 concept of climate risk. Bonn, Germany.

Glover, J., Denk, M., Bourrier, F., Volkwein, A., Gerber, W., 2012. Measuring the kinetic energy dissipation effects of rock fall attenuating systems with video analysis. In 12th Congress INTERPRAEVENT (Vol. 1, pp. 151-160).

Goetz, Guthrie, R.H., Brenning, A., 2015. Forest harvesting is associated with increased landslide activity during an extreme rainstorm on Vancouver Island, Canada. Natural Hazards and Earth System Science 15, 1311–1330. https://doi.org/10.5194/nhess-15-1311-2015

Goetz, J.N., Brenning, A., Petschko, H., Leopold, P., 2015. Evaluating machine learning and statistical prediction techniques for landslide susceptibility modeling. Computers & Geosciences 81, 1–11. https://doi.org/10.1016/j.cageo.2015.04.007

Gsteiger, P., 1993. Steinschlagschutzwald. Ein Beitrag zur Abgrenzung, Beurteilung und Bewirtschaftung. Schweiz. Z. Forstwes, 144(2), 115-132.

Gubler, H., 1987. Measurements and modelling of snow avalanche speeds. IAHS Publ, 162, 405-420.

Holmgren, P., 1994. Multiple flow direction algorithms for runoff modelling in grid based elevation models: an empirical evaluation. Hydrological Processes, 8:327–334.

Horton, P., Jaboyedoff, M., Rudaz, B., and Zimmermann, M., 2013. Flow-R, a model for susceptibility mapping of debris flows and other gravitational hazards at a regional scale. Natural Hazards and Earth System Science, 13:869–885.

Huber, A., Kofler, A., Fischer, J.-T., Kleemayr, K., 2017. DAKUMO. Technical report, Federal Research and Training Centre for Forests, Natural Hazards and Landscape, Innsbruck, Austria.

Huber, A., Perzl, F., Fromm, R., 2015. Verbesserung der Beurteilung der Waldflächen mit direkter Objektschutzwirkung durch Modellierung von Massenbewegungsprozessen (GRAVIPROMOD). Project Report, Austrian Research Centre for Forests (BFW).

Hungr, O., Leroueil, S., Picarelli, L., 2013. The Varnes classification of landslide types, an update. Landslides 11, 167–194. https://doi.org/10.1007/s10346-013-0436-y

Intergovernmental Panel on Climate Change (IPCC), 2014. Climate Change 2014: Impacts, Adaptation, and Vulnerability. Part A: Global and Sectoral Aspects. Contribution of Working Group II to the Fifth Assessment Report of the Intergovernmental Panel on Climate Change. Cambridge, UK; New York, NY, USA.

International Standard Organisation, 2018. ISO 31000:2018 (en) Risk management, 2nd ed. ISO/TC 262.

Jaboyedoff, M., Dudt, J. P., Labiouse, V., 2005: An attempt to refine rockfall hazard zoning based on the kinetic energy, frequency and fragmentation degree, Nat. Hazards Earth Syst. Sci., 5, 621–632, doi:10.5194/nhess-5-621-2005.

Jacobs, L., Dewitte, O., Poesen, J., Maes, J., Mertens, K., Sekajugo, J., Kervyn, M., 2016. Landslide characteristics and spatial distribution in the Rwenzori Mountains, Uganda. Journal of African Earth Sciences. https://doi.org/10.1016/j.jafrearsci.2016.05.013

Jahn, J., 1988. Entwaldung und Steinschlag (pp. 185-198). EAFV/Eigenverlag.

Jóhannesson, T., Gauer, P., Issler, P., Lied, K., 2009. The design of avalanche protection dams: Recent practical and theoretical developments. Brussels, European Communities. 195pp. ISBN 978-92-79-08885-8

Korup, O., Clague, J.J., 2009. Natural hazards, extreme events, and mountain topography. Quaternary Science Reviews, 28(11-12), 977-990.

Kuriakose, S.L., van Beek, L.P.H., van Westen, C.J., 2009. Parameterizing a physically based shallow landslide model in a data poor region. Earth Surface Processes and Landforms 34, 867–881. https://doi.org/10.1002/esp.1794

Lateltin, O., Tripet, J., Boell, A., Bonnard, C., Hansen, J., Krummenacher, B., Loat, R., Bernard, L., Rouiller, J., Schneider, J., 1997. Empfehlungen 1997–Berücksichtigung der Massenbewegungsgefahren bei raumwirksamen Tätigkeiten. Bundesamt für Raumplanung, Bundesamt für Wasserwirtschaft, Bundesamt für Umwelt, Wald und Landschaft (Hrsg.), Bern.

Lingua, E., Bettella, F., Pividori, M., Marzano, R., Garbarino, M., Piras, M., Kobal, M., Berger, F., 2020. The Protective Role of Forests to Reduce Rockfall Risks and Impacts in the Alps Under a Climate Change Perspective, Climate Change, Hazards and Adaptation Options. Springer, pp. 333-347.

Mikoš, M., 2013. Risk Management and Mountain Natural Hazards., in: Bekic, D. (Ed.), 2nd Professional & Scientific Conference Water Management Days 2013 “Progress Through Science.” Zagreb, Croatia, pp. 245–268.

Mölk, M., Rieder, B., 2017. Rockfall hazard zones in Austria. Experience, problems and solutions in the development of a standardised procedure: Steinschlag-Gefahrenzonen in Österreich. Erfahrungen, Probleme und Lösungsansätze bei der Entwicklung einer standardisierten Vorgangsweise. Geomechanics and Tunneling, 10(1), 24-33.

Moos, C., Bebi, P., Graf, F., Mattli, J., Rickli, C., Schwarz, M., 2016. How does forest structure affect root reinforcement and susceptibility to shallow landslides?: A Case Study in St Antönien, Switzerland. Earth Surface Processes and Landforms 41, 951–960. https://doi.org/10.1002/esp.3887

Oswald, V., 2020. Auswirkungen des Schutzwaldes auf Steinschlagmodellierungen in Vals. Sensitivitätsanalyse in Rockyfor3D und RAMMS: ROCKFALL. Master thesis, Universität Innsbruck, Innsbruck, 122 pp.

Perzl, F., Den Outer, J., Rössler, M., 2014. GRAVIPROFOR – Schutzwaldkulisse in der forstlichen Raumplanung. Methodik – Datengrundlagen für die Modellierung von Waldflächen mit Lawinen- und Steinschlag-Objektschutzfunktion. Projektsbericht im Auftrag des Bundesministeriums für Land- und Forstwirtschaft, Umwelt und Wasserwirtschaft im Rahmen der Technischen Hilfe des österreichischen Programms LE 07-13 mit Unterstützung von Bund, Ländern und der Europäischen Union. Teilbericht. V2. Zahl: BMLFUW-LE.1.3-7/0020-II/5/2012.

Perzl, F., Huber, A., 2014. Verbesserung der Erfassung der Schutzwaldkulisse für die forstliche Raumplanung - Synthese und Zusammenfassung. Project Report, Austrian Research Centre for Forests (BFW).

Perzl, F., Walter, D., 2012. Die Lawinen-Schutzwirkung des Waldes im Klimawandel. AlpineSPACE Projekt MANFRED: Management strategies to adapt Alpine Space forests to climate change risks, Deliverables.

Petschko, H., Brenning, A., Bell, R., Goetz, J., Glade, T., 2014. Assessing the quality of landslide susceptibility maps – case study Lower Austria. Natural Hazards and Earth System Science 14, 95–118. https://doi.org/10.5194/nhess-14-95-2014

Rapin, F., 2002. A new scale for avalanche intensity. In International Snow Science Workshop, volume 2, pages 103–110.

Reichenbach, P., Rossi, M., Malamud, B.D., Mihir, M., Guzzetti, F., 2018. A review of statistically-based landslide susceptibility models. Earth-Science Reviews 180, 60–91. https://doi.org/10.1016/j.earscirev.2018.03.001

Scheidl, C., Heiser, M., Vospernik, S., Lauss, E., Perzl, F., Kofler, A., Kleemayr; K., Bettella, F., Lingua, E., Garbarino, M., Skudnik, M., Trappmann, D., Berger, F., 2020. Assessing the protective role of alpine forests against rockfall at regional scale. European Journal of Forest Research, 1-12.

Schmaltz, E.M., Steger, S., Glade, T., 2017. The influence of forest cover on landslide occurrence explored with spatio-temporal information. Geomorphology 290, 250–264. https://doi.org/10.1016/j.geomorph.2017.04.024

Schmaltz, E.M., Van Beek, L.P.H., Bogaard, T.A., Kraushaar, S., Steger, S., Glade, T., 2019. Strategies to improve the explanatory power of a dynamic slope stability model by enhancing land cover parameterisation and model complexity. Earth Surface Processes and Landforms 44, 1259–1273. https://doi.org/10.1002/esp.4570

Schneebeli, M., Bebi, P., 2004. Snow and avalanche control. In Burley, J., Evans, J., and Youngquist, J.A. (eds.), Encyclopedia of Forest Sciences. Elsevier, 397-402.

Seefelder, C. de L.N., Koide, S., Mergili, M., 2017. Does parameterization influence the performance of slope stability model results? A case study in Rio de Janeiro, Brazil. Landslides 14, 1389–1401. https://doi.org/10.1007/s10346-016-0783-6

Sidle, R.C., Ochiai, H., 2006. Landslides: processes, prediction, and land use. American Geophysical Union. xxxxx

Steger, S., 2017. Spatial analysis and statistical modelling of landslide susceptibility - pitfalls and solutions. Dissertation Thesis. University of Vienna, Vienna, Austria. http://othes.univie.ac.at/47980/

Steger, S., Brenning, A., Bell, R., Glade, T., 2017. The influence of systematically incomplete shallow landslide inventories on statistical susceptibility models and suggestions for improvements. Landslides 14, 1767–1781. https://doi.org/10.1007/s10346-017-0820-0

Steger, S., Brenning, A., Bell, R., Petschko, H., Glade, T., 2016. Exploring discrepancies between quantitative validation results and the geomorphic plausibility of statistical landslide susceptibility maps. Geomorphology 262, 8–23. https://doi.org/10.1016/j.geomorph.2016.03.015

Steger, S., Kofler, C., 2019. Statistical Modeling of Landslides: Landslide Susceptibility and Beyond, in: Pourghasemi, H.R., Gokceoglu, C. (Eds.), Spatial Modeling in GIS and R for Earth and Environmental Sciences. Elsevier, pp. 519–546.

Steger, S., Mair, V., Kofler, C., Pittore, M., Zebisch, M., Schneiderbauer, S., 2020. A statistical exploratory analysis of inventoried slide-type movements for South Tyrol (Italy), in: Proceedings of the 5th World Landslide Forum, 2-6 November 2020, Kyoto, Japan. Springer, Kyoto.

Stokes, A., Salin, F., Kokutse, A. D., Berthier, S., Jeannin, H., Mochan, S., ... & Fourcaud, T. (2005). Mechanical resistance of different tree species to rockfall in the French Alps. Plant and soil, 278(1-2), 107-117.

Takeuchi, Y., Nishimura, K., Patra, A., 2018. Observations and numerical simulations of the braking effect of forests on large-scale avalanches. Annals of Glaciology, 59(77), 50-58.

Teich, M., Bartelt, P., Grêt-Regamey, A., Bebi, P., 2012. Snow avalanches in forested terrain: influence of forest parameters, topography, and avalanche characteristics on runout distance. Arctic, Antarctic, and Alpine Research 44(4), 509-519.

Teich, M., Fischer, J.-T., Feistl, T., Bebi, P., Christen, M., Grêt-Regamey, A., 2014. Computational snow avalanche simulation in forested terrain. Natural Hazards and Earth System Sciences 14(8), 2233-2248.

Toppe, R., 1987. Terrain models: a tool for natural hazard mapping. IAHS, Publication, 162.

United Nations Office for Disaster Risk Reduction (UNDRR), 2009. UNISDR Terminology on Disaster Risk Reduction.

Volkwein, A., Schellenberg, K., Labiouse, V., Agliardi, F., Berger, F., Bourrier, F., Dorren, L.K., Gerber, W., Jaboyedoff, M., 2011. Rockfall characterisation and structural protection-a review. Natural Hazards and Earth System Sciences, 11, 2617-2651.

Wasser, B., Frehner, M., 1996. Minimale Pflegemassnahmen für Wälder mit Schutzfunktion. Wegleitung, Bundesamt für Umwelt, Wald und Landschaft (BUWAL), Bern, pp. 122.